

A METHOD OF ESTIMATING THE APOGEE AND PERIGEE ERROR  
INCURRED IN ESTABLISHING THE ORBIT OF A SPIN-STABILIZED VEHICLE

by

Benjamin J. Garland

Thesis submitted to the Graduate Faculty of the

Virginia Polytechnic Institute

in candidacy for the degree of

MASTER OF SCIENCE

in

AERONAUTICAL ENGINEERING

June 1960

Blacksburg, Virginia

II. TABLE OF CONTENTS

| CHAPTER  | PAGE |
|--|------|
| I. TITLE . . . . .   | 1    |
| II. TABLE OF CONTENTS . . . . .  | 2    |
| III. LIST OF FIGURES AND TABLE . . . . .   | 4    |
| IV. LIST OF SYMBOLS . . . . .  | 6    |
| V. INTRODUCTION . . . . .  | 8    |
| VI. GENERAL CONSIDERATIONS . . . . .   | 10   |
| VII. ANALYSIS . . . . .  | 13   |
| A. Error in Injection Radius . . . . .   | 14   |
| B. Error in Injection Velocity . . . . .   | 17   |
| C. Error in Injection Angle . . . . .  | 21   |
| D. Summary of Equations for Errors in Injection<br>Radius, Velocity, and Angle . . . . . | 25   |
| E. Errors in Apogee Altitude . . . . .   | 30   |
| F. Errors in Perigee Altitude . . . . .  | 35   |
| VIII. PROCEDURE FOR CALCULATING ERRORS . . . . .   | 41   |
| IX. ACCURACY OF PARTIAL DERIVATIVES . . . . .  | 44   |
| X. SAMPLE CALCULATIONS . . . . .   | 47   |
| XI. CONCLUSIONS . . . . .  | 52   |
| XII. ACKNOWLEDGMENTS . . . . .   | 53   |
| XIII. REFERENCES . . . . .   | 54   |
| XIV. VITA . . . . .  | 56   |

| CHAPTER  | PAGE |
|--|------|
| XV. APPENDICES . . . . .   | 57   |
| A. Development of the Ballistic Equations in the Forms<br>Used . . . . .         | 57   |
| B. Development of the Equation for the Error in the<br>Injection Angle . . . . . | 64   |
| C. Evaluation of Partial Derivatives . . . . .                                   | 73   |

III. LIST OF FIGURES AND TABLE

| FIGURE   | PAGE |
|--|------|
| 1. Definition of Terms Which are Used in Theory. . . . .   | 15   |
| 2. Rate of Change of $r_1/r_0$ With Respect to $V_0/V_{c,0}$ for<br>Values of $V_0/V_{c,0}$ and $\gamma_0$ . . . . .     | 18   |
| 3. Rate of Change of $r_1/r_0$ With Respect to $\theta_0$ for Values<br>of $V_0/V_{c,0}$ and $\gamma_0$ . . . . .        | 19   |
| 4. Rate of Change of $V_1/V_{c,0}$ With Respect to $V_0/V_{c,0}$<br>for Values of $V_0/V_{c,0}$ and $\gamma_0$ . . . . . | 22   |
| 5. Rate of Change of $V_1/V_{c,0}$ With Respect to $\gamma_0$ for<br>Values of $V_0/V_{c,0}$ and $\gamma_0$ . . . . .    | 23   |
| 6. Rate of Change of $\theta_0$ With Respect to $\gamma_0$ for Values<br>of $V_0/V_{c,0}$ and $\gamma_0$ . . . . .       | 26   |
| 7. Rate of Change of $\theta_0$ With Respect to $V_0/V_{c,0}$ for<br>Values of $V_0/V_{c,0}$ and $\gamma_0$ . . . . .    | 27   |
| 8. Rate of Change of $t/T_{c,0}$ With Respect to $\gamma_0$ for<br>Values of $V_0/V_{c,0}$ and $\gamma_0$ . . . . .      | 28   |
| 9. Rate of Change of $t/T_{c,0}$ With Respect to $V_0/V_{c,0}$<br>for Values of $V_0/V_{c,0}$ and $\gamma_0$ . . . . .   | 29   |
| 10. Rate of Change of $r_a/r_1$ With Respect to $V_i/V_{c,i}$<br>for Values of $V_i/V_{c,i}$ . . . . .                   | 33   |
| 11. Rate of Change of $r_p/r_1$ With Respect to $\gamma_i$ for Values<br>of $V_i/V_{c,i}$ . . . . .                      | 34   |
| 12. Rate of Change of $r_a/r_1$ With Respect to $\gamma_i$ for Values<br>of $V_i/V_{c,i}$ . . . . .                      | 38   |

| FIGURE  | PAGE |
|---|------|
| 13. Conditions at Burnout of the Next-to-the-Last Stage . . . . .                                 | 48   |
| 14. Probable Distribution of Apogee and Perigee Altitudes of<br>the Scout Vehicle . . . . .       | 50   |
| 15. Addition of Velocity Vectors . . . . .  | 63   |
| 16. Relationship of $\gamma_1$ to $\psi$ and $\theta_{\Delta t}$ . . . . .                        | 63   |
| 17. Relation of Angles Influencing the Angle of Attack at<br>Ignition of the Last Stage . . . . . | 67   |
| TABLE . . . . .   | 45   |

IV. LIST OF SYMBOLS

|                                     |   |
|-------------------------------------|---|
| a                                   | semimajor axis of ellipse, ft                                     |
| b                                   | semiminor axis of ellipse, ft                                     |
| A,B,C,D,E,<br>F,G,H,I               | terms defined in equations (20a), (20b), and (20c)                |
| A',B',C',D',<br>E',F'               | terms defined in equation (25)                                    |
| A'',B'',C'',D'',<br>E'',F'',G'',H'' | terms defined in equations (34a) and (34b)                        |
| e                                   | numerical eccentricity  |
| $\epsilon$                          | gravitational constant  |
| h                                   | altitude above surface of earth, ft                               |
| K                                   | curvature, radians/ft   |
| m                                   | mass of body, lb-sec <sup>2</sup> /ft                             |
| r                                   | radius, ft  |
| R                                   | radius of earth (20,926,435 ft)                                   |
| s                                   | arc distance traveled during the burning of the last<br>stage, ft |
| t                                   | time required to travel from a point to apogee, sec               |
| $T_{c,j}$                           | period of circular orbit of radius $r_j$ , sec                    |
| V                                   | velocity, ft/sec  |
| $V_{c,j}$                           | velocity for circular orbit at radius $r_j$ , ft/sec              |
| $V_e$                               | exhaust velocity relative to the vehicle, ft/sec                  |
| w                                   | weight, lb  |
| x                                   | distance traveled over the earth's surface, ft                    |

|                     |  |
|---------------------|--|
| $\alpha$            | angle of attack, radians   |
| $\gamma$            | flight-path angle, radians (unless noted otherwise)  |
| $\gamma_p$          | the change of flight-path angle due to disturbances<br>of the spin-stabilized last stage, radians  |
| $\theta$            | central angle between a point and apogee, radians  |
| $\theta_{\Delta t}$ | the central angle between the ignition of the last stage<br>and the peak of the actual ascent trajectory (due to<br>change in time necessary to reach the peak), radians |
| $\mu$               | gravitational parameter for earth ( $1.407528 \times 10^{16}$ ft <sup>3</sup> /sec <sup>2</sup> )  |
| $\sigma$            | standard deviation   |
| $\phi$              | the angle between the longitudinal body axis and the local<br>horizon at the peak of the ascent trajectory with zero<br>errors, radians                                  |
| $\psi$              | the angle between the local horizon at the actual peak of<br>the ascent trajectory and the tangent to the flight path<br>at ignition of the last stage, radians          |
| $\omega$            | thrust misalignment, radians   |
| Subscripts          |  |
| o                   | conditions at burnout of the next-to-last stage  |
| l                   | conditions at ignition of the last stage   |
| i                   | conditions at burnout of the last stage (injection)  |
| j                   | refers to any general condition  |
| a                   | apogee   |
| p                   | perigee  |
| A                   | peak of intended ascent trajectory   |
| $\delta$            | change during burning of the last stage  |

## V. INTRODUCTION

A necessary part of any study concerning the launching of a satellite vehicle is an analysis of the effect of errors present during the launching upon the final orbit which is to be achieved. This information may be used to determine the accuracies (in velocity, altitude, flight-path angle at burnout of the next-to-last stage, thrust of the last stage, etc.) which must be maintained to insure an orbit which is satisfactory for the purpose of the satellite. If these accuracies are fixed (and this is the normal situation), this analysis will give the error in the orbit which should be expected.

In the case to be considered here, there exists a coast period between the burnout of the next-to-last stage and the ignition of the last stage. This period may be treated by use of the ballistic equations which require that the altitude at burnout of the next-to-last stage should be great enough to allow the neglect of aerodynamic drag. The last stage is then ignited at the peak of the ascent trajectory and provides the velocity increment necessary to place the satellite into orbit.

There is no provision for velocity control in the vehicle so the only manner in which the injection altitude and velocity may be varied is by changing the launch angle of the initial stage and ignition time of the subsequent stages. It should be noted that the majority of orbits of interest will not be circular.

Previously the Martin Company (ref. 1) has studied this problem using machine calculated trajectories. In this study, several parameters



were varied separately, by small amounts, and trajectories calculated. This type of study requires a large amount of time and is limited to a particular vehicle. Gedeon and Dawler (ref. 2) have studied the effect of injection parameters upon orbits which are not limited to near-circular conditions while Benegra (ref. 3) has studied the same problem for near-circular orbits. These last two studies do not consider how the errors present at burnout of the last stage develop, and consequently a different method must be used to determine this. Since only a few of the possible orbits may be considered as near circular, the second study is of little use in the present analysis.

In determining the errors for the more general case, the present analysis makes use of the partial derivatives of the solutions to the equations of motion for a particle in a central force field. Charts of these partial derivatives are presented for a wide range of initial conditions which greatly reduce the amount of work required to evaluate the errors in the apogee and perigee altitudes.

## VI. GENERAL CONSIDERATIONS

The type of vehicle which is of interest in the present analysis is a multistage rocket. The particular vehicle is the Scout which is a four-stage solid-fuel rocket. Each of the stages except the last is provided with controls which are capable of regulating the direction that the vehicle points and the time of ignition of each stage. Aerodynamic controls (fins) are used on the first stage and reaction controls (hydrogen-peroxide rockets) are used on the second and third stages although the type of control is unimportant in this analysis. There is no control over the velocity increment of each stage. The guidance system which operates the controls is located in the next-to-last stage.

The last two stages are locked together until the ignition of the last stage and the controls in the next-to-last stage are used to align the longitudinal axis of the last two stages parallel to the local horizontal at the peak of the ascent trajectory. Immediately before the ignition of the last stage, the last stage is spun about its longitudinal axis which stabilizes it when it is not connected to the preceding stage.

The trajectory of the vehicle may be divided into four portions. The first portion includes the trajectory between the launching of the vehicle and the burnout of the next-to-last stage. The presence of aerodynamic and control forces during this portion of the trajectory result in equations of motion which cannot be solved in closed form. An IBM 704 was used to solve the three degree-of-freedom equations of motion. The three degree-of-freedom considered are translations in

the vertical plane and a rotation about the pitch axis of the vehicle. The errors in altitude, velocity, and flight-path angle at burnout of the next-to-last stage were found using a number of machine calculated trajectories in which individual quantities such as total impulse, weight, thrust alinement and guidance accuracy of each stage were varied seperately. The errors in altitude, velocity, and flight-path angle at burnout of the next-to-last stage were found by the root-mean-square method using the errors caused by the individual variation of these quantities.

The second portion of the trajectory is the coast period between the burnout of the next-to-last stage and the ignition of the last stage. This portion of the trajectory is assumed to take place at an altitude which is sufficiently large so that any aerodynamic forces present are negligible. The control forces required to orient the last two stages prior to ignition of the last stage are assumed to rotate the last two stages about their center of gravity without altering their trajectory. The trajectory of the last two stages during the coast period can be treated using the ballistic equations because of the assumption that the aerodynamic and control forces are negligible.

The third portion of the trajectory occurs during the burning of the last stage and is treated by an approximate method. A treatment of the errors during this period using the method of Sohn (ref. 4), a better approximation than the method used here, would be more complicated and not of sufficiently improved accuracy to justify the additional complications.

The fourth portion of the trajectory is the orbit after burnout of the last stage, or injection. This portion is treated using the

orbital equations. The only quantities of interest to this analysis are the apogee and perigee altitudes.

The first portion of the trajectory is studied using machine calculations. This analysis is concerned with the last three portions of the trajectory.

## VII. ANALYSIS

The errors in the trajectory after burnout of the next-to-last stage are treated using a convergent Taylor's series. The general form of a series of this type for a function of  $m$  variables is given by reference 5 as

$$f(x_1 + k_1, x_2 + k_2, \dots, x_m + k_m) = \sum_{n=0}^{\infty} \frac{1}{n!} \left( k_1 \frac{\partial}{\partial x_1} + k_2 \frac{\partial}{\partial x_2} + \dots + k_m \frac{\partial}{\partial x_m} \right)^{(n)} f(x_1, x_2, \dots, x_m) \quad (1)$$

where the symbolic notation with the index  $n$  in parentheses denotes the result of multiplying out the operator formally and then operating on the function. This series exists if  $f(x_1, x_2, \dots, x_m)$  has partial derivatives of all orders and if

$$\lim_{n \rightarrow \infty} \frac{1}{n!} \left( k_1 \frac{\partial}{\partial x_1} + k_2 \frac{\partial}{\partial x_2} + \dots + k_m \frac{\partial}{\partial x_m} \right)^{(n)} f(x_1, x_2, \dots, x_m)_{(x_1 + \theta_n k_1, x_2 + \theta_n k_2, \dots, x_m + \theta_n k_m)} = 0$$

for  $(0 < \theta_n < 1)$

where the notation indicates that the partial derivatives in this limit are evaluated at the point  $(x_1 + \theta_n k_1, x_2 + \theta_n k_2, \dots, x_m + \theta_n k_m)$ .

If the constants  $k_1, k_2, \dots, k_m$  are defined to be small changes or errors in the corresponding variables then equation (1) can be written as

$$f(x_1 + \Delta x_1, x_2 + \Delta x_2, \dots, x_m + \Delta x_m) = \sum_{n=0}^{\infty} \frac{1}{n!} \left( \Delta x_1 \frac{\partial}{\partial x_1} + \Delta x_2 \frac{\partial}{\partial x_2} + \dots + \Delta x_m \frac{\partial}{\partial x_m} \right)^{(n)} f(x_1, x_2, \dots, x_m) \quad (2)$$

If only the first two terms of the series are considered, equation (2) becomes

$$f(x_1 + \Delta x_1, x_2 + \Delta x_2, \dots, x_m + \Delta x_m) - f(x_1, x_2, \dots, x_m) = \left( \Delta x_1 \frac{\partial}{\partial x_1} + \Delta x_2 \frac{\partial}{\partial x_2} + \dots + \Delta x_m \frac{\partial}{\partial x_m} \right) f(x_1, x_2, \dots, x_m) \quad (3)$$

The error in the function is defined as

$$\Delta f(x_1, x_2, \dots, x_m) = f(x_1 + \Delta x_1, x_2 + \Delta x_2, \dots, x_m + \Delta x_m) - f(x_1, x_2, \dots, x_m)$$

and therefore

$$\Delta f(x_1, x_2, \dots, x_m) = \left( \Delta x_1 \frac{\partial}{\partial x_1} + \Delta x_2 \frac{\partial}{\partial x_2} + \dots + \Delta x_m \frac{\partial}{\partial x_m} \right) f(x_1, x_2, \dots, x_m) \quad (4)$$

This is the general form which will be used to determine the errors in the functions of interest.

The notation used in the analysis is illustrated in figure 1.

#### A. Errors in Injection Radius ( $\Delta r_1$ )

The injection radius ( $r_1$ ) is a function of the following quantities (see eq. (A-10)):

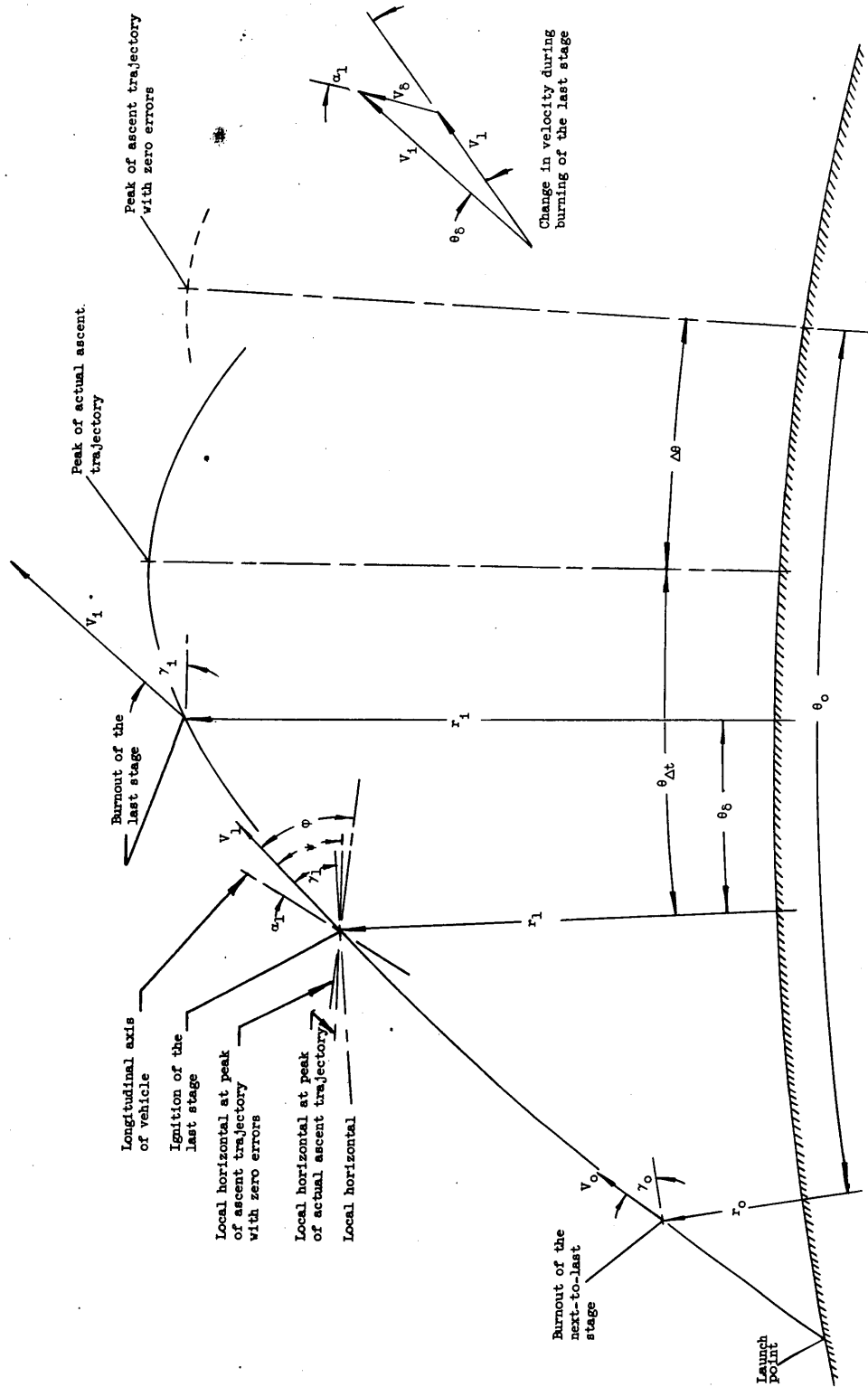


Figure 1.- Definition of terms which are used in the theory.

$$r_1 = f(r_0, V_0, \gamma_0, r_8) \quad (5)$$

The error in the injection radius, equal to the change in injection altitude, is found, using equation (4), to be

$$\Delta r_1 = \frac{\partial r_1}{\partial r_0} \Delta r_0 + \frac{\partial r_1}{\partial V_0} \Delta V_0 + \frac{\partial r_1}{\partial \gamma_0} \Delta \gamma_0 + \frac{\partial r_1}{\partial r_8} \Delta r_8 \quad (6)$$

The injection radius is the radius at ignition of the last stage ( $r_1$ ) plus the change in radius during the burning of the last stage ( $r_8$ )

$$r_1 = r_1 + r_8 \quad (7)$$

The only manner that  $r_8$  could be effected by small errors in  $r_0$ ,  $V_0$ , and  $\gamma_0$  would be through changes in  $r_1$ , resulting in changes in the aerodynamic drag and the force of gravity during the burning of the last stage. The aerodynamic drag has already been assumed negligible. The last stage travels almost horizontally during this period so that gravity has only a small effect upon the distance traveled and the extremely small change in the force of gravity caused by small changes in  $r_0$ ,  $V_0$ , and  $\gamma_0$  is completely negligible.

With these considerations equation (6) becomes

$$\Delta r_1 = \Delta r_0 + \frac{\partial r_1}{\partial V_0} \Delta V_0 + \frac{\partial r_1}{\partial \gamma_0} \Delta \gamma_0 + \Delta r_8 \quad (8)$$

For the Scout vehicle the largest value of  $\Delta r_0$  will be no greater than 1 nautical mile as indicated by a series of machine calculated trajectories. The last stage travels almost horizontally during its period of burning and as a result, the change in altitude during this



period will be less than 5 percent of the distance traveled. In most cases, this change will be less than 5 miles. If the minimum injection altitude is greater than 150 nautical miles, then the total error in  $r_1$  caused by  $\Delta r_0$  and  $\Delta \gamma_0$  will be less than 4 percent and can be neglected. When  $\Delta r_0$  and  $\Delta \gamma_0$  are neglected, equation (8) becomes

$$\Delta r_1 = \frac{\partial r_1}{\partial V_0} \Delta V_0 + \frac{\partial r_1}{\partial \gamma_0} \Delta \gamma_0 \quad (9)$$

This equation may be rewritten in a form which will be simpler to use. Since  $\Delta r_0$  is small ( $r_0$  and  $V_{c,0}$  are considered to be constant) equation (9) becomes

$$\Delta r_1 = \frac{r_0}{V_{c,0}} \frac{\partial(r_1/r_0)}{\partial(V_0/V_{c,0})} \Delta V_0 + r_0 \frac{\partial(r_1/r_0)}{\partial \gamma_0} \Delta \gamma_0 \quad (10)$$

when expressed in ratio form.

Expressing the partial derivatives in this form has the advantage of eliminating  $r_0$  as a variable. The equations of these partial derivatives are given in appendix C (eqs. (C1) and (C2)) and presented in figures 2 and 3.

#### B. Errors in Injection Velocity ( $\Delta V_i$ )

The injection velocity is a function of the following quantities (eq. (A33))

$$V_i = f(r_0, V_0, \gamma_0, \phi_1, V_\delta) \quad (11)$$

The error in  $V_i$  can be expressed as

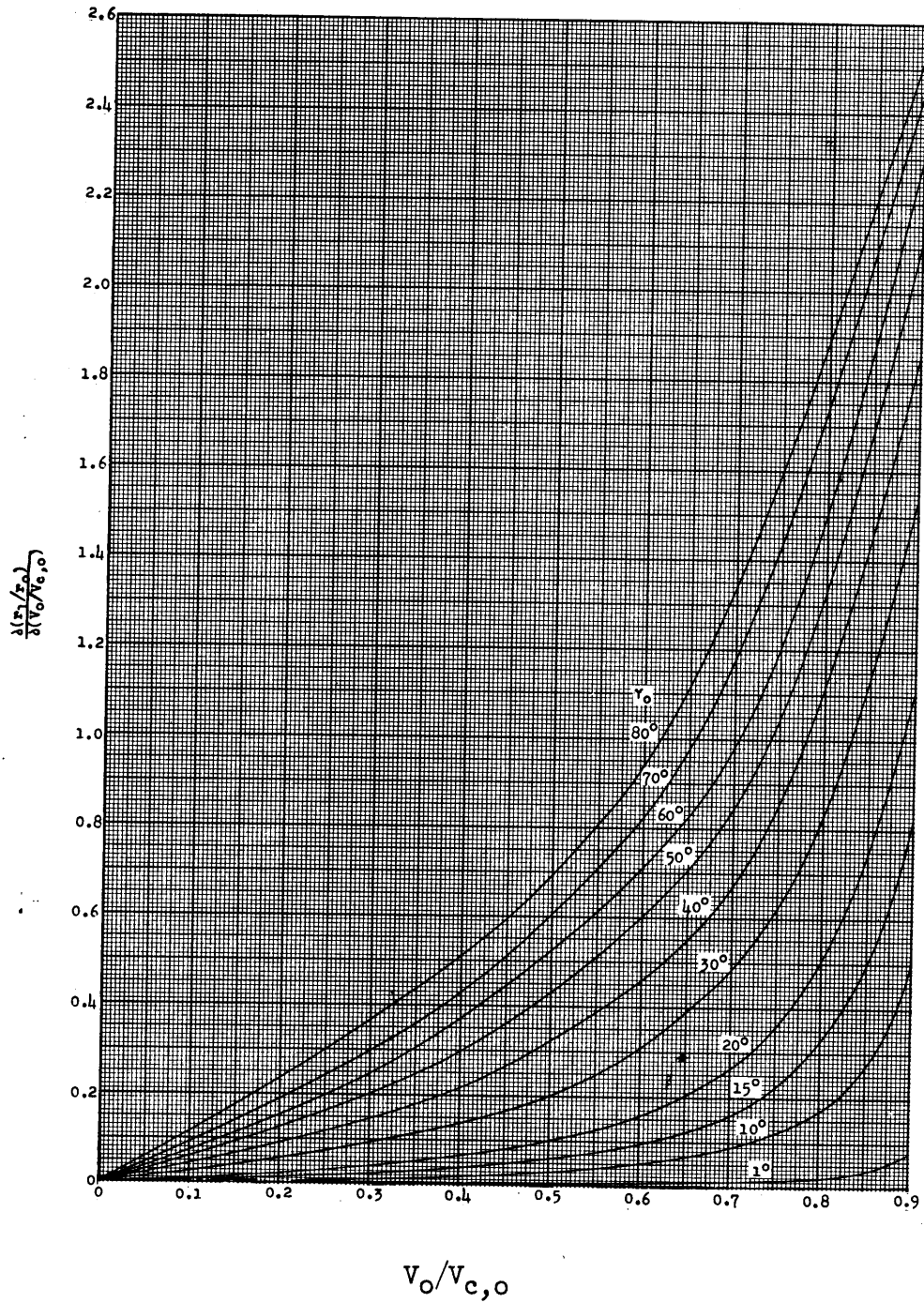


Figure 2.- Rate of change of  $r_1/r_0$  with respect to  $V_0/V_{c,0}$  for values of  $V_0/V_{c,0}$  and  $\gamma_0$ .

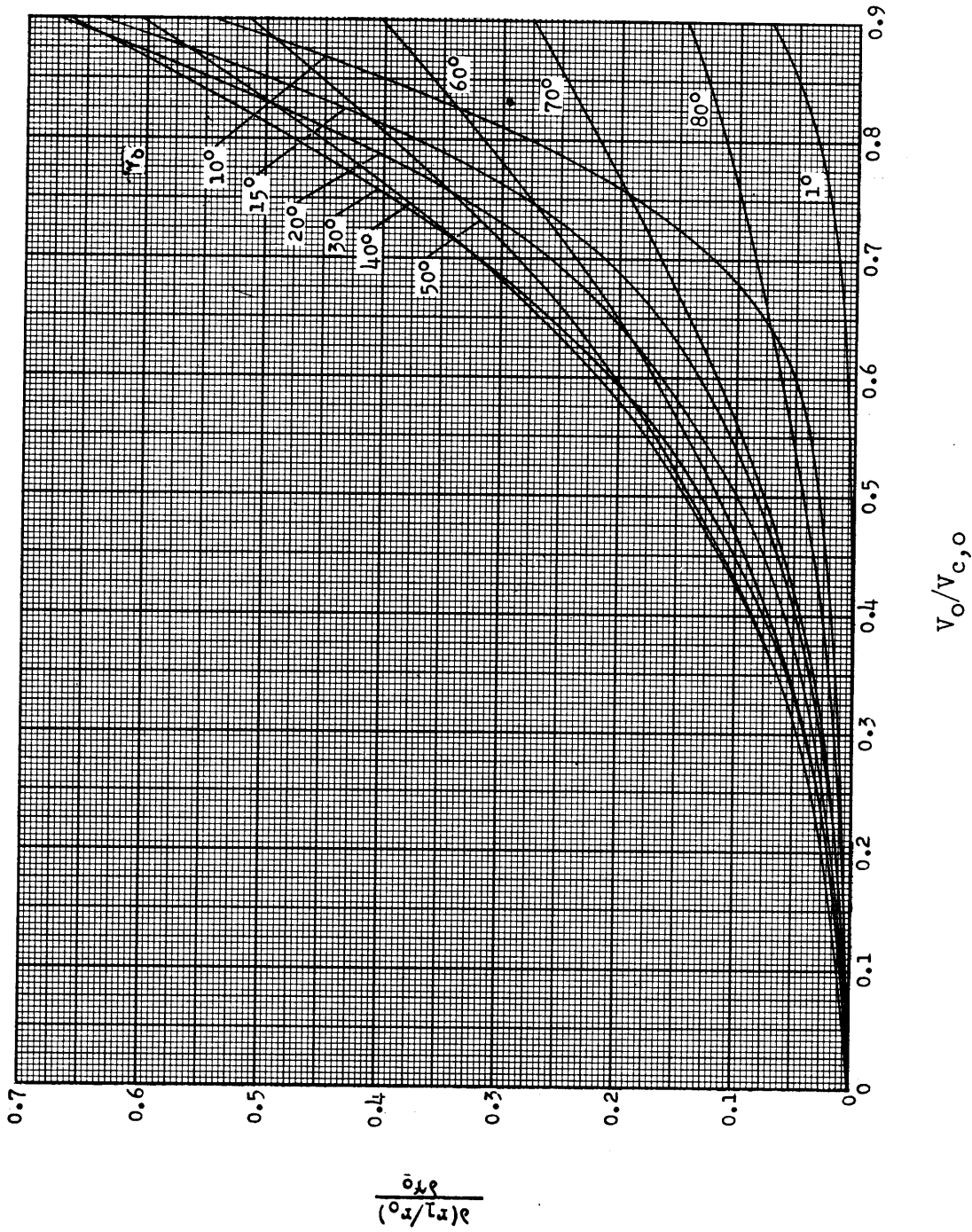


Figure 3.- Rate of change of  $r_1/r_0$  with respect to  $\theta_0$  for values of  $V_0/V_{c,0}$  and  $\gamma_0$ .

$$\Delta V_1 = \frac{\partial V_1}{\partial r_0} \Delta r_0 + \frac{\partial V_1}{\partial V_0} \Delta V_0 + \frac{\partial V_1}{\partial \gamma_0} \Delta \gamma_0 + \frac{\partial V_1}{\partial \phi_1} \Delta \phi_1 + \frac{\partial V_1}{\partial V_8} \Delta V_8 \quad (12)$$

The injection velocity ( $V_1$ ) is the vector sum of the velocity at ignition of the last stage ( $V_1$ ) and the velocity increment of the last stage ( $V_8$ ). The simple scalar addition neglecting angularity of these velocities will cause less than 0.1 percent change in  $V_1$  for the range of velocities and angles of interest ( $10,000 < V_1 < 20,000$ ;  $5,000 < V_8 < 15,000$ ;  $-5^\circ < \alpha < 5^\circ$ ), so that

$$V_1 \approx V_1 + V_8 \quad (13)$$

Small changes in  $r_0$ ,  $V_0$ , and  $\gamma_0$  will have a negligible effect upon  $V_8$  for the same reasons that they had a negligible effect upon  $r_8$ .

With these considerations equation (12) may be written as

$$\Delta V_1 = \frac{\partial V_1}{\partial r_0} \Delta r_0 + \frac{\partial V_1}{\partial V_0} \Delta V_0 + \frac{\partial V_1}{\partial \gamma_0} \Delta \gamma_0 + \frac{\partial V_8}{\partial \phi_1} \Delta \phi_1 + \Delta V_8 \quad (14)$$

This equation may be simplified by considering the size of the following:

$\frac{\partial V_1}{\partial r_0} \Delta r_0 \approx 0$  that is, aerodynamic drag is neglected and the effect of a very small change in the force of gravity caused by a small change in  $r_0$  can also be neglected.

$\frac{\partial V_8}{\partial \phi} \Delta \phi \approx 0$  that is,  $V_8$  depends only slightly upon  $\phi_1$  and  $\Delta \phi_1$  is small so that their product is negligible.

With these assumptions equation (14) becomes

$$\Delta V_1 = \frac{\partial V_1}{\partial V_0} \Delta V_0 + \frac{\partial V_1}{\partial \gamma_0} \Delta \gamma_0 + \Delta V_8 \quad (15)$$

This equation may now be written in a form similar to equation (10), or

$$\Delta V_1 = \frac{\partial(V_1/V_{c,0})}{\partial(V_0/V_{c,0})} \Delta V_0 + V_{c,0} \frac{\partial(V_1/V_{c,0})}{\partial \gamma_0} \Delta \gamma_0 + \Delta V_8 \quad (16)$$

The partial derivatives in this equation are given in appendix C (eqs. (C3) and (C9)) and are presented in figures 4 and 5.

### C. Errors in Injection Angle ( $\Delta \gamma_1$ )

The injection error which remains to be considered is the error in the flight-path angle at injection ( $\Delta \gamma_1$ ). Figure 1 shows that the injection flight-path angle is given by the relation

$$\gamma_1 = \gamma_1 + \gamma_8 + \gamma_p + \theta_8 \quad (17)$$

where, in equation (17)

$\gamma_1$  is the flight-path angle at ignition of the last stage.

$\gamma_8$  is the change in flight-path angle during the thrusting of the last stage, if the last stage is treated as a particle.

$\gamma_p$  is the change in flight-path angle during the thrusting of the spin stabilized last stage caused by disturbances such as thrust misalignment and initial pitch rate assuming the angle of attack to be zero.

$\theta_8$  is the central angle change during thrusting of the last stage.

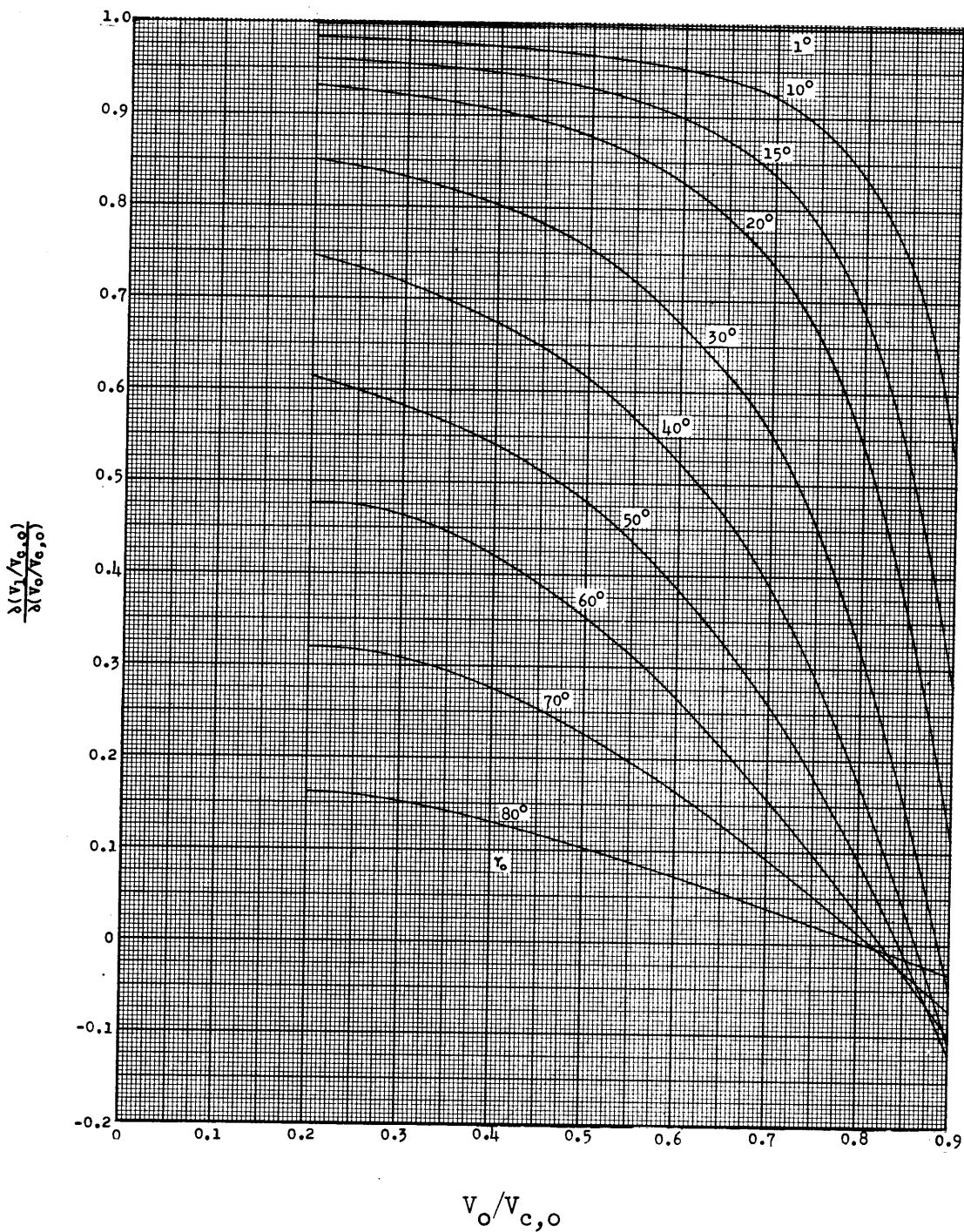


Figure 4.- Rate of change of  $V_1/V_{c,0}$  with respect to  $V_0/V_{c,0}$  for values of  $V_0/V_{c,0}$  and  $\gamma_0$ .

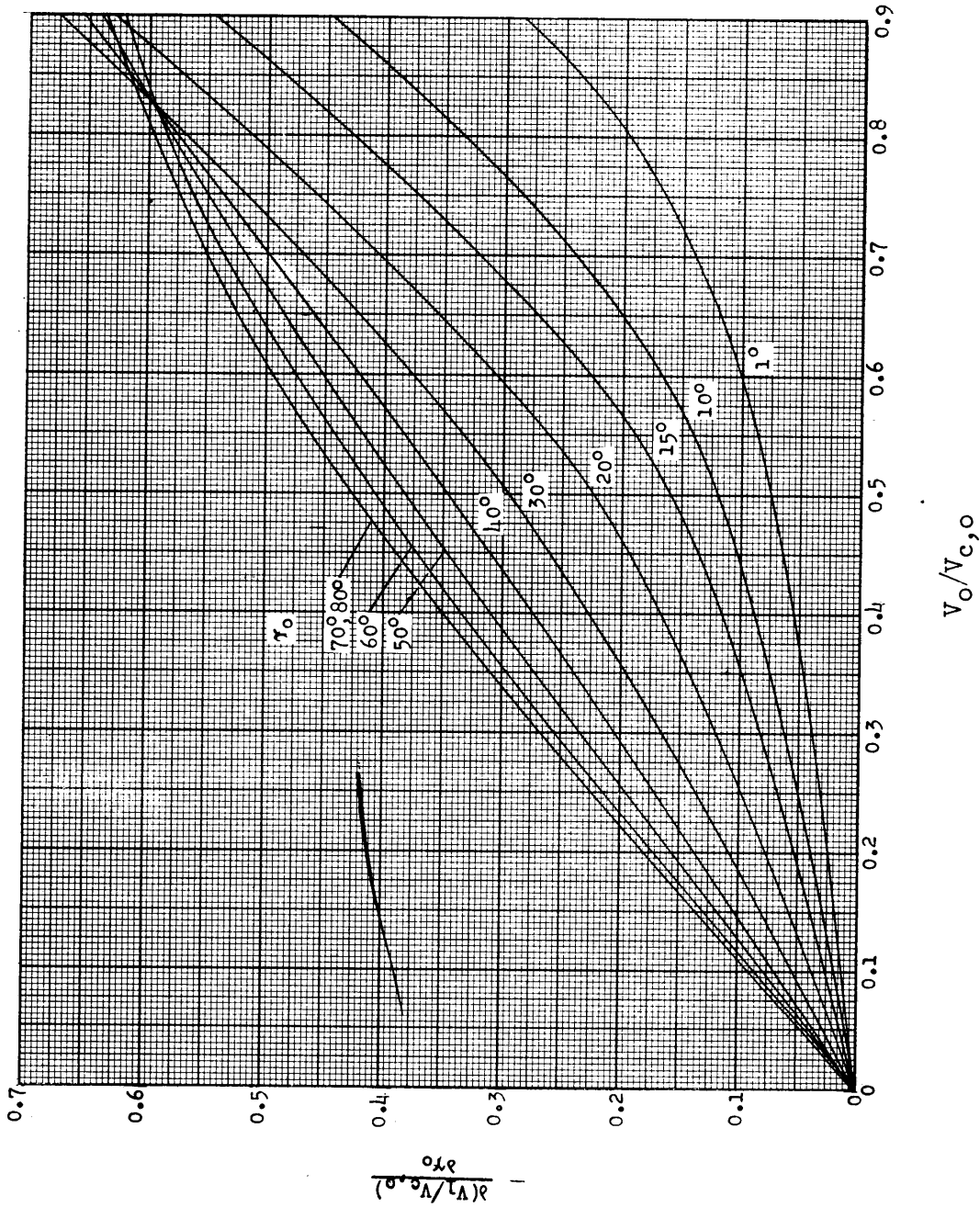


Figure 5.- Rate of change of  $V_1/V_{c,0}$  with respect to  $V_0/V_{c,0}$  for values of  $V_0/V_{c,0}$  and  $\gamma_0$ .

Thus, it follows that the error in  $\gamma_1$  is

$$\Delta\gamma_1 = \frac{\partial\gamma_1}{\partial\gamma_1} \Delta\gamma_1 + \frac{\partial\gamma_1}{\partial\gamma_8} \Delta\gamma_8 + \frac{\partial\gamma_1}{\partial\gamma_p} \Delta\gamma_p + \frac{\partial\gamma_1}{\partial\theta_8} \Delta\theta_8 \quad (18)$$

but equation (17) shows that

$$\frac{\partial\gamma_1}{\partial\gamma_1} = \frac{\partial\gamma_1}{\partial\gamma_8} = \frac{\partial\gamma_1}{\partial\gamma_p} = \frac{\partial\gamma_1}{\partial\theta_8} = 1$$

so that

$$\Delta\gamma_1 = \Delta\gamma_1 + \Delta\gamma_8 + \Delta\gamma_p + \Delta\theta_8 \quad (19)$$

The equations for the various terms in this equation are derived in appendix B. When these are substituted into equation (19) and simplified, by neglecting second order terms, the equation for  $\Delta\gamma_1$  becomes

$$\begin{aligned} \Delta\gamma_1 = & \left\{ \frac{T_{c,o}}{V_{c,o}} \frac{1}{1-e} \left[ e - \frac{V_8}{V_1} \right] \frac{V_1}{r_1} \frac{\partial(t/T_{c,o})}{\partial(V_o/V_{c,o})} + \frac{1}{V_{c,o}} \frac{V_8}{V_1} \frac{\partial\theta_o}{\partial(V_o/V_{c,o})} \right\} \Delta V_o + \\ & \left\{ T_{c,o} \frac{1}{1-e} \left[ e - \frac{V_8}{V_1} \right] \frac{V_1}{r_1} \frac{\partial(t/T_{c,o})}{\partial\gamma_o} + \frac{V_8}{V_1} \frac{\partial\theta}{\partial\gamma_o} \right\} \Delta\gamma_o + \frac{V_8}{V_1} \Delta\theta + \\ & \frac{\partial\gamma_8}{\partial\omega} \Delta\omega + \frac{\partial\gamma_8}{\partial\gamma_1} \Delta\gamma_1 \end{aligned} \quad (B19)$$

The partial derivatives  $\frac{\partial\theta_o}{\partial\gamma_o}$ ,  $\frac{\partial\theta_o}{\partial(V_o/V_{c,o})}$ ,  $\frac{\partial(t/T_{c,o})}{\partial\gamma_o}$ , and  $\frac{\partial(t/T_{c,o})}{\partial(V_o/V_{c,o})}$

are developed in appendix C (eqs. (C5), (C6), (C7), and (C8)) and are



presented in figures 6, 7, 8, and 9. The partial derivatives  $\frac{\partial \gamma_8}{\partial \omega}$  and  $\frac{\partial \gamma_8}{\partial \gamma_1}$  can be found by using information given by the method of Buglia, Young, Timmons, and Brinkworth (ref. 6).

D. Summary of Equations for Errors in Injection Radius,  
Velocity, and Angle

For convenience, equations (10), (16), and (B-19) are summarized below

$$\Delta r_1 = A \Delta V_0 + B \Delta \gamma_0 \quad (20a)$$

$$\Delta V_1 = C \Delta V_0 + D \Delta \gamma_0 + \Delta V_8 \quad (20b)$$

$$\Delta \gamma_1 = E \Delta V_0 + F \Delta \gamma_0 + G \Delta \omega + H \Delta \gamma_1 + I \Delta \varphi \quad (20c)$$

where

$$A = \frac{r_0}{v_{c,o}} \frac{\partial(r_1/r_0)}{\partial(v_0/v_{c,o})}$$

$$B = r_0 \frac{\partial(r_1/r_0)}{\partial \gamma_0}$$

$$C = \frac{\partial(v_1/v_{c,o})}{\partial(v_0/v_{c,o})}$$

$$D = v_{c,o} \frac{\partial(v_1/v_{c,o})}{\partial \gamma_0}$$

$$E = \frac{1}{v_{c,o}} \frac{v_8}{v_1} \frac{\partial \theta}{\partial(v_0/v_{c,o})} + \frac{T_{c,o}}{v_{c,o}} \frac{1}{1 - e} \left[ e - \frac{v_8}{v_1} \right] \frac{v_1}{r_1} \frac{\partial(t/T_{c,o})}{\partial(v_0/v_{c,o})}$$

$$F = \frac{v_8}{v_1} \frac{\partial \theta}{\partial \gamma_0} + T_{c,o} \frac{1}{1 - e} \left[ e - \frac{v_8}{v_1} \right] \frac{v_1}{r_1} \frac{\partial(t/T_{c,o})}{\partial \gamma_0}$$

$$G = \frac{\partial \gamma_8}{\partial \omega}$$

$$H = \frac{\partial \gamma_8}{\partial \gamma_1}$$

$$I = \frac{v_8}{v_1}$$

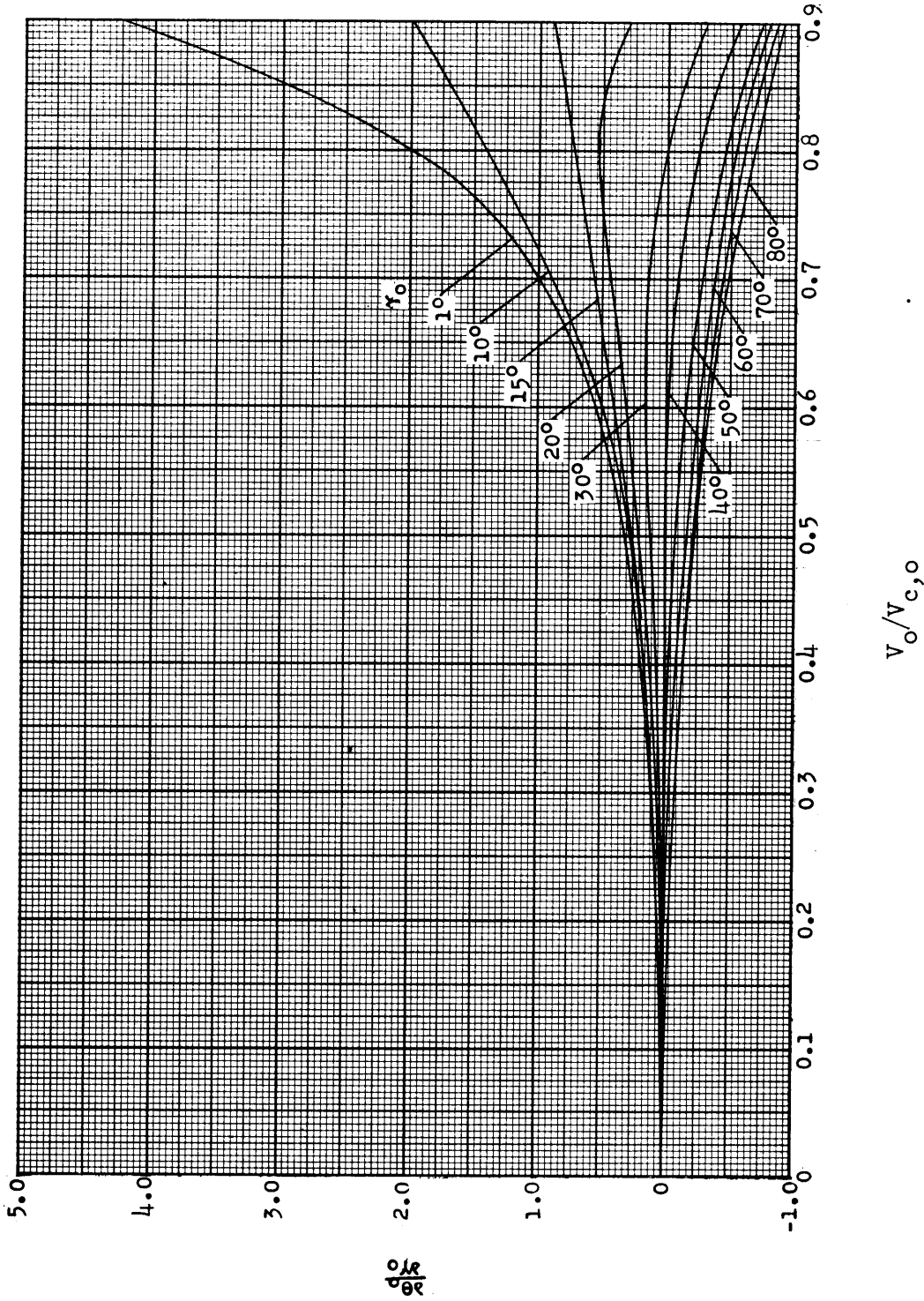


Figure 6.- Rate of change of  $\theta_0$  with respect to  $\gamma_0$  for values of  $V_0/V_{c,0}$  and  $\gamma_0$ .

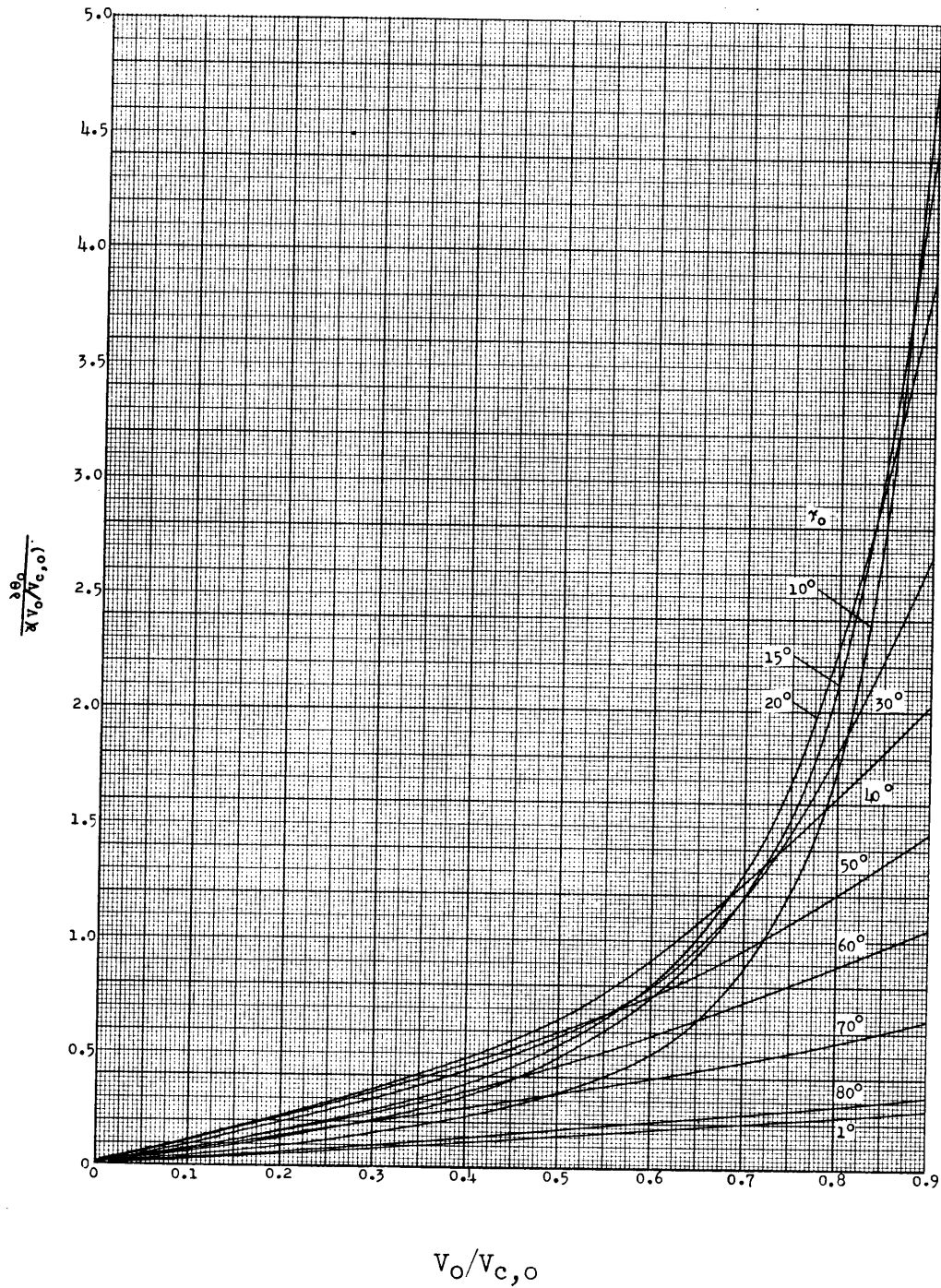


Figure 7.- Rate of change of  $\theta_0$  with respect to  $V_0/V_{c,0}$  for values of  $V_0/V_{c,0}$  and  $\gamma_0$ .

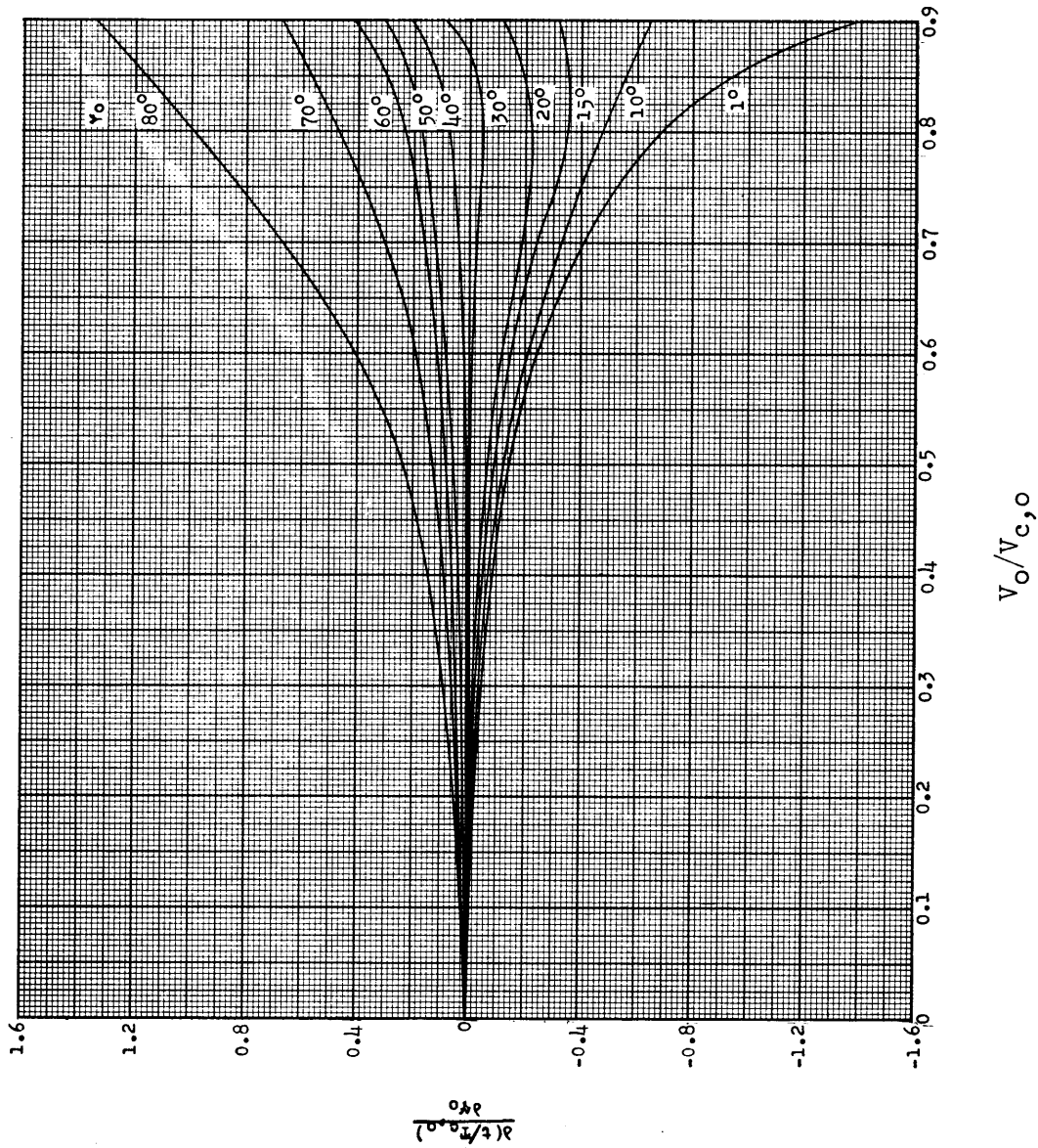


Figure 8.- Rate of change of  $t/T_{c,0}$  with respect to  $\gamma_0$  for values of  $V_0/V_{c,0}$  and  $\gamma_0$ .

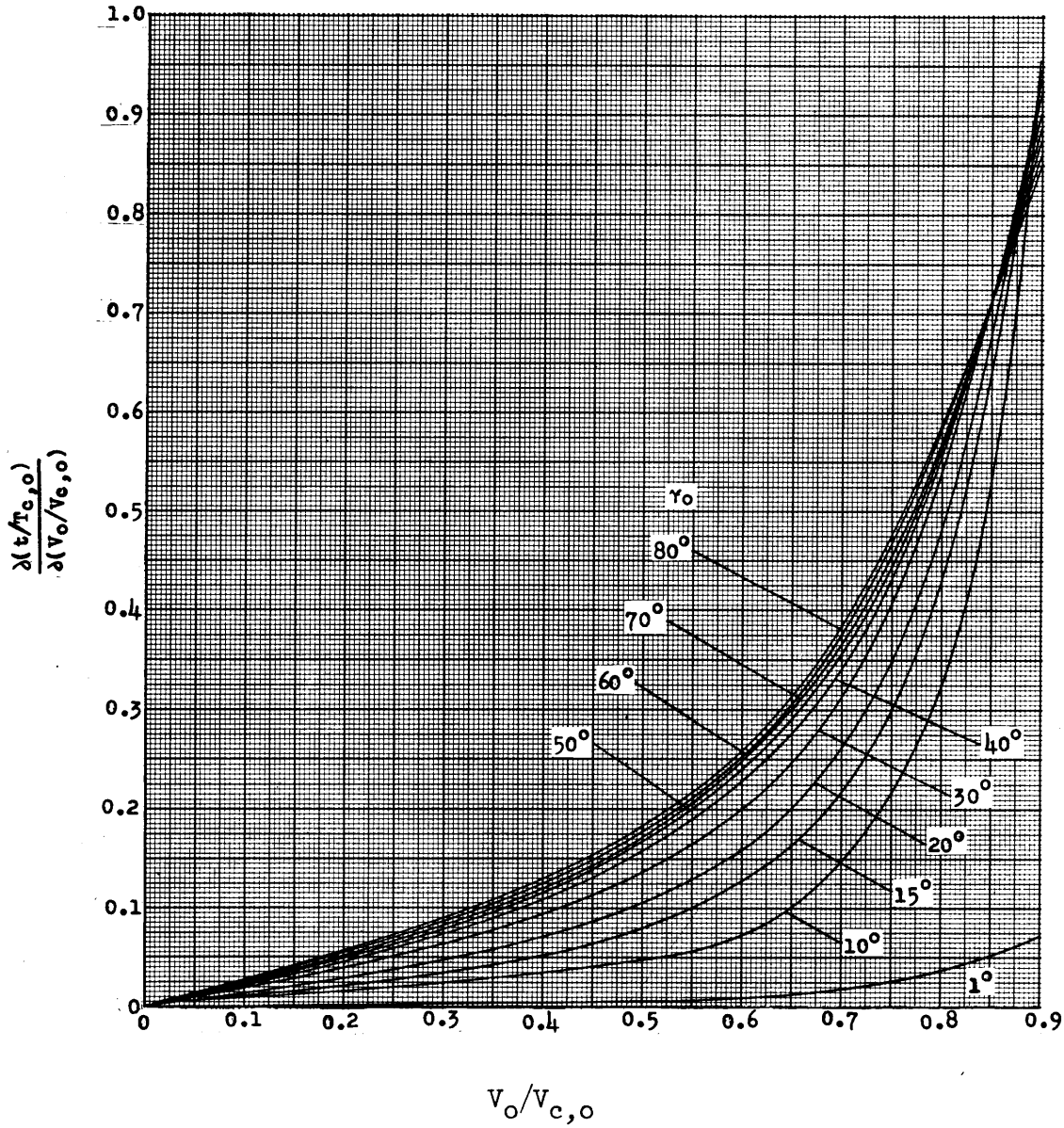


Figure 9.- Rate of change of  $t/T_{c,0}$  with respect to  $V_0/V_{c,0}$  for values of  $V_0/V_{c,0}$  and  $\gamma_0$ .

These equations are useful only if the values of  $\Delta V_0$ ,  $\Delta \gamma_0$ ,  $\Delta V_8$ ,  $\Delta \omega$ ,  $\Delta \dot{\gamma}_1$ , and  $\Delta \phi$  are known. In practice, only the standard deviations of these quantities will be known. The standard deviation is a measure of the dispersion of a quantity. The probability that the dispersion of a quantity will be less than a given fraction of the standard deviation may be found in tables, such as those in reference 7.

The relation between the standard deviation of the known quantities  $[\sigma(\Delta V_0), \sigma(\Delta \gamma_0), \sigma(\Delta V_8), \sigma(\Delta \omega), \sigma(\dot{\gamma}_1), \text{ and } \sigma(\Delta \phi)]$  and the standard deviation of the unknown quantities  $[\sigma(\Delta r_1), \sigma(\Delta V_1), \text{ and } \sigma(\Delta \gamma_1)]$  is given in reference 8. The standard deviations of  $\Delta r_1$ ,  $\Delta V_1$ , and  $\Delta \gamma_1$  are

$$\sigma(\Delta r_1) = \left\{ A^2 [\sigma(\Delta V_0)]^2 + B^2 [\sigma(\Delta \gamma_0)]^2 \right\}^{1/2} \quad (21a)$$

$$\sigma(\Delta V_1) = \left\{ C^2 [\sigma(\Delta V_0)]^2 + D^2 [\sigma(\Delta \gamma_0)]^2 + [\sigma(\Delta V_8)]^2 \right\}^{1/2} \quad (21b)$$

$$\sigma(\Delta \gamma) = \left\{ E^2 [\sigma(\Delta V_0)]^2 + F^2 [\sigma(\Delta \gamma_0)]^2 + G^2 [\sigma(\Delta \omega)]^2 + H^2 [\sigma(\Delta \dot{\gamma}_1)]^2 + I^2 [\sigma(\Delta \phi)]^2 \right\}^{1/2} \quad (21c)$$

#### E. Errors in Apogee Altitude ( $\Delta h_a$ )

The values of  $\Delta r_1$ ,  $\Delta V_1$ , and  $\Delta \gamma_1$  given by equations (20a), (20b), and (20c) are used to determine the errors in apogee altitude. Since the apogee altitude and apogee radius are related to the earth's radius by the relation

$$h_a = R - r_a$$

it is apparent that

$$\Delta h_a = \Delta r_a$$

hence  $\Delta h_a$  and  $\Delta r_a$  may be used interchangeably.

The equation for the apogee altitude ( $h_a$ ) is developed in appendix A and is

$$h_a = \frac{(V_i/V_{c,i})^2 \cos^2 \gamma_i}{1 - e} r_i - R \quad (A16)$$

where

$$e = \left\{ 1 + (\cos^2 \gamma_i) \left( \frac{V_i}{V_{c,i}} \right)^2 \left[ \left( \frac{V_i}{V_{c,i}} \right)^2 - 2 \right] \right\}^{1/2} \quad (A18)$$

In equations (A16) and (A18) the circular velocity, at the injection radius ( $V_{c,i}$ ), is fixed by the value of the injection radius ( $r_i$ ).

Now the error in the apogee altitude ( $\Delta h_a$ ) is given by equation (4) to be

$$\Delta h_a = \frac{\partial r_a}{\partial r_i} \Delta r_i + \frac{r_i}{V_{c,i}} \frac{\partial(r_a/r_i)}{\partial(V_i/V_{c,i})} \Delta V_i + r_i \frac{\partial(r_a/r_i)}{\partial \gamma_i} \Delta \gamma_i \quad (22)$$

This equation may be simplified by noting that

$$\frac{\partial r_a}{\partial r_i} = 1$$

so that equation (22) becomes

$$\Delta h_a = \Delta r_i + \frac{r_i}{V_{c,i}} \frac{\partial(r_a/r_i)}{\partial(V_i/V_{c,i})} \Delta V_i + r_i \frac{\partial(r_a/r_i)}{\partial \gamma_i} \Delta \gamma_i \quad (23)$$

It is necessary to modify this equation to account for the physical behavior of the problem which is revealed by a study of equations (A16) and (A18). A change in  $r_i$  may cause an increase or a decrease in  $h_a$ . An increase in  $V_i$  will increase the eccentricity of the orbit ( $e$ ) causing the denominator of equation (A16) to decrease and also will increase the numerator resulting in an increase in  $h_a$ . Similarly, a decrease in  $V_i$

will cause a decrease in  $h_a$ . The terms involving  $\gamma_1$  will always be positive so that any variation of  $\gamma_1$  from its nominal value of zero will increase  $e$  and an increase in  $h_a$  will result. Thus equation (23) may be rewritten as

$$\Delta h_a = \Delta r_i + \frac{r_i}{v_{c,i}} \frac{\partial(r_a/r_i)}{\partial(v_i/v_{c,i})} + \text{sgn}(\Delta\gamma_1)r_i \frac{\partial(r_a/r_i)}{\partial\gamma_1} \Delta\gamma_1 \quad (24)$$

where  $\text{sgn}(\Delta\gamma_1)$  means the sign of  $\Delta\gamma_1$  (or  $\text{sgn} \Delta\gamma_1 = \Delta\gamma_1/|\Delta\gamma_1|$ ).

When equations (20a), (20b), and (20c) are substituted into equation (29) and terms are combined, it becomes

$$\Delta h_a = A' \Delta V_0 + B' \Delta\gamma_0 + C' \Delta\omega + D' \Delta\dot{\gamma}_1 + E' \Delta\varphi + F' \Delta V_8 \quad (25)$$

where

$$A' = A + \frac{r_i}{v_{c,i}} \frac{\partial(r_a/r_i)}{\partial(v_i/v_{c,i})} C + \text{sgn}(\Delta\gamma_1)r_i \frac{\partial(r_a/r_i)}{\partial\gamma_1} E$$

$$B' = B + \frac{r_i}{v_{c,i}} \frac{\partial(r_a/r_i)}{\partial(v_i/v_{c,i})} D + \text{sgn}(\Delta\gamma_1)r_i \frac{\partial(r_a/r_i)}{\partial\gamma_1} F$$

$$C' = \text{sgn}(\Delta\gamma_1)r_i \frac{\partial(r_a/r_i)}{\partial\gamma_1} G$$

$$D' = \text{sgn}(\Delta\gamma_1)r_i \frac{\partial(r_a/r_i)}{\partial\gamma_1} H$$

$$E' = \text{sgn}(\Delta\gamma_1)r_i \frac{\partial(r_a/r_i)}{\partial\gamma_1} I$$

$$F' = \frac{r_i}{v_{c,i}} \frac{\partial(r_a/r_i)}{\partial(v_i/v_{c,i})}$$

The partial derivatives  $\frac{\partial(r_a/r_i)}{\partial(v_i/v_{c,i})}$  and  $\frac{\partial(r_a/r_i)}{\partial\gamma_1}$  are given in

appendix C (eqs. (C46) and (C47)) and presented in figures 10 and 11.



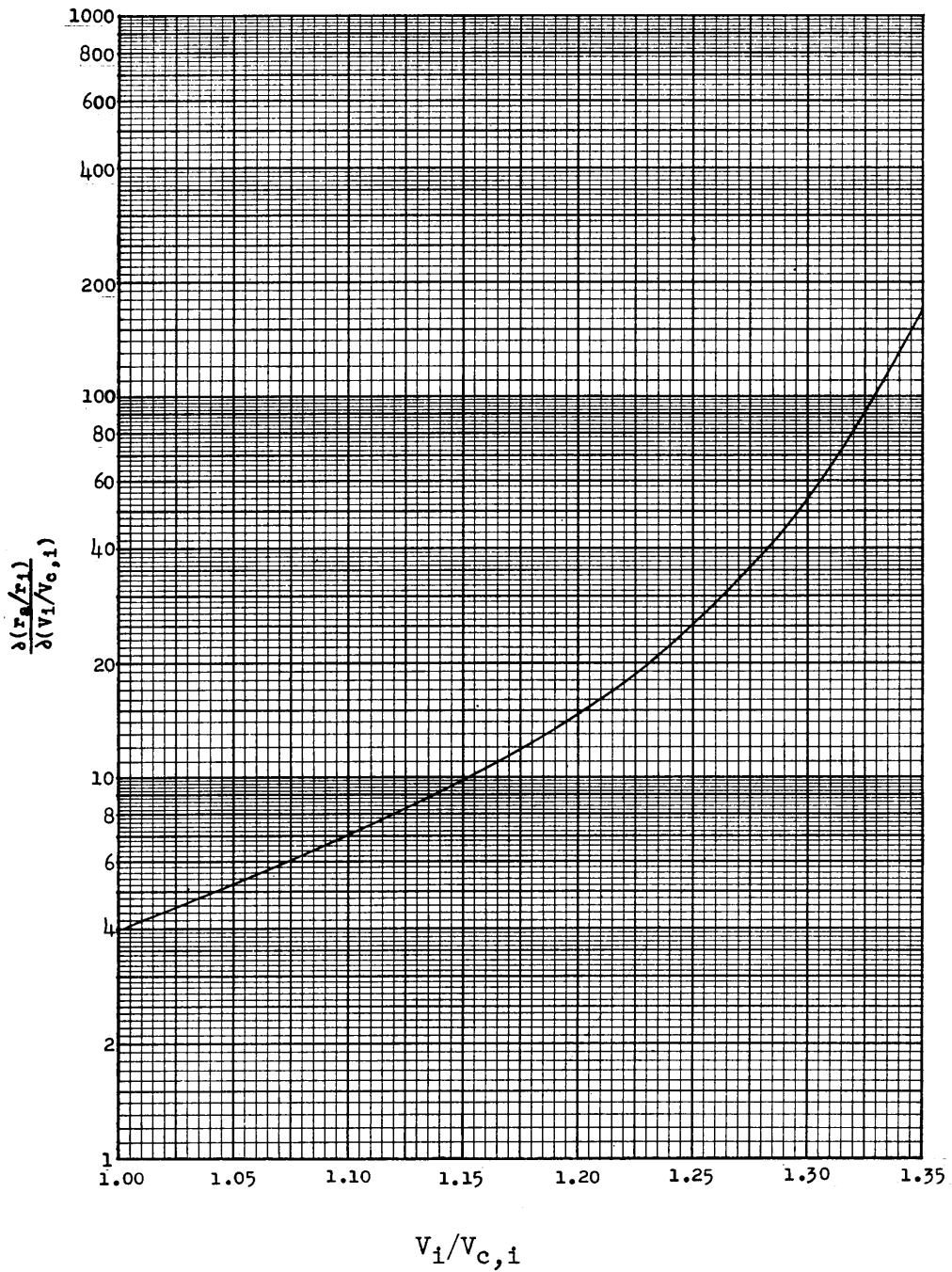


Figure 10.- Rate of change of  $r_a/r_1$  with respect to  $V_1/V_{c,i}$  for values of  $V_1/V_{c,i}$ .

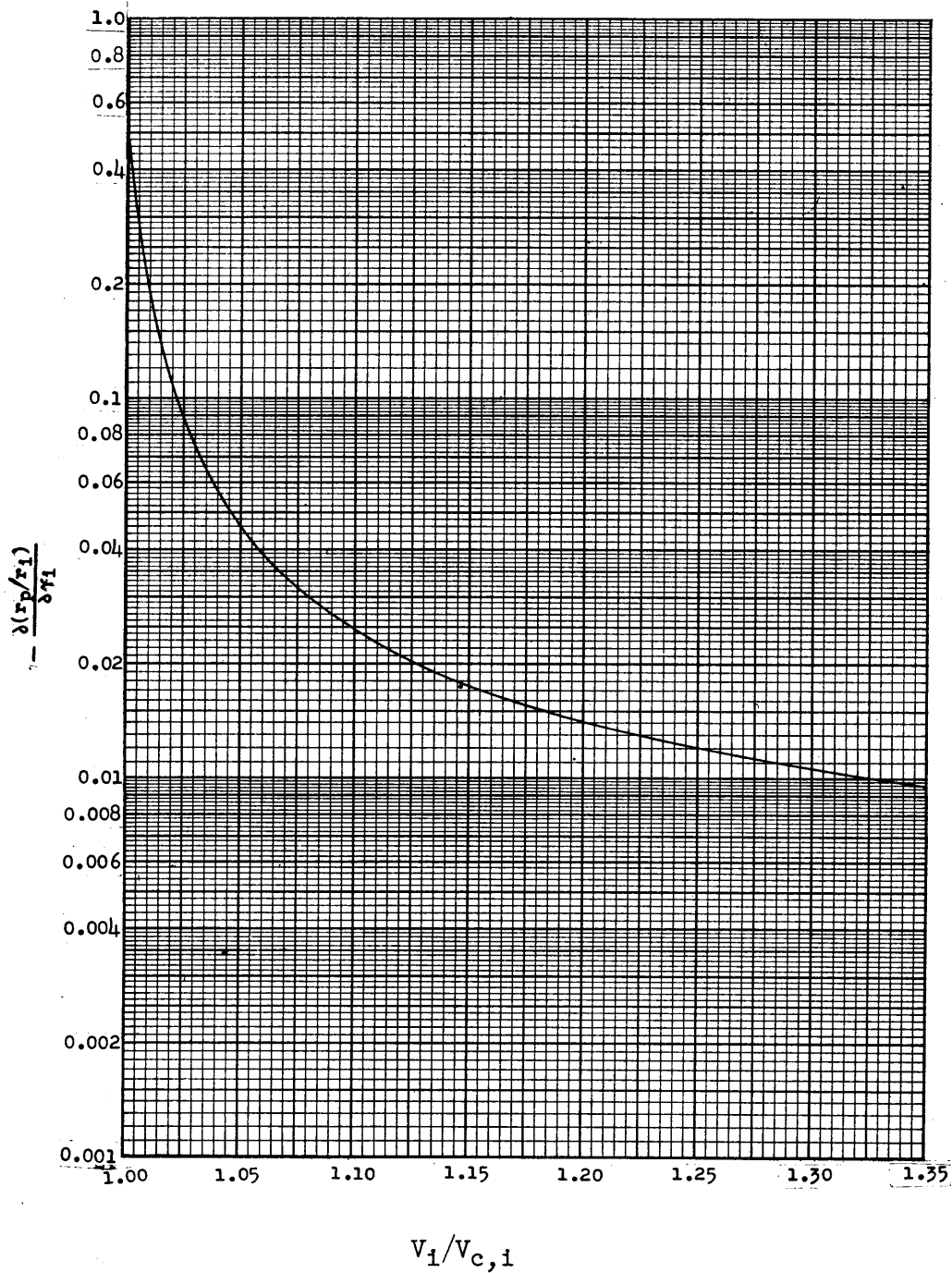


Figure 11.- Rate of change of  $r_p/r_i$  with respect to  $\gamma_i$  for values of  $V_1/V_{c,i}$ .

The standard deviation of the error in apogee altitude  $[\sigma(\Delta h_a)]$  must be treated for the reasons given previously concerning the injection parameters. In a similar manner, the standard deviation of the error in apogee altitude is

$$\sigma(\Delta h_a) = \left\{ (A')^2 [\sigma(\Delta V_0)]^2 + (B')^2 [\sigma(\Delta \gamma_0)]^2 + (C')^2 [\sigma(\Delta \omega)]^2 + (D')^2 [\sigma(\Delta \dot{\gamma}_1)]^2 + (E')^2 [\sigma(\Delta \varphi)]^2 + (F')^2 [\sigma(\Delta V_8)]^2 \right\}^{1/2} \quad (26)$$

#### F. Errors in Perigee Altitude ( $\Delta h_p$ )

The error in the perigee altitude ( $\Delta h_p$ ) is found in a manner similar to that used in the preceding section. The error in the perigee altitude can be written as

$$\Delta h_p = \Delta r_1 + \frac{r_1}{V_{c,i}} \frac{\partial(r_p/r_1)}{\partial(V_1/V_{c,i})} \Delta V_1 + r_1 \frac{\partial(r_p/r_1)}{\partial \gamma_1} \Delta \gamma_1 \quad (27)$$

since the equation for the perigee altitude is

$$h_p = \frac{(V_1/V_{c,i}) \cos^2 \gamma_1}{1 + e} r_1 - R \quad (A17)$$

Errors in  $r_1$  may cause an increase or a decrease in  $h_p$  as in the case of  $h_a$ . However, any change in  $\gamma_1$  from its nominal value of zero will cause a decrease in  $h_p$  which is the opposite of its influence upon  $h_a$ . The effect of changes in  $V_1$  must be considered more thoroughly. Since  $\gamma_1 \approx 0$ , then  $\cos \gamma_1 \approx 1$  and

$$h_p = \frac{(V_1/V_{c,i})^2}{1 + e} r_1 - R \quad (28)$$

where

$$e = \frac{V_i^2}{V_{c,i}} - 1 \quad \text{for } V_i > V_{c,i} \quad (29a)$$

or

$$e = 1 - \frac{V_i^2}{V_{c,i}} \quad \text{for } V_i < V_{c,i} \quad (29b)$$

The substitution of equation (29a) into equation (28) yields

$$h_p = r_1 - R \quad (30)$$

so that

$$\frac{\partial(r_p/r_1)}{\partial(V_i/V_{c,i})} = 0 \quad (31)$$

When equation (29b) is substituted into equation (28) the resulting equation is

$$h_p = \frac{(V_i/V_{c,i})^2}{2 - (V_i/V_{c,i})^2} r_1 - R \quad (32)$$

In the first case where  $V_i > V_{c,i}$ ,  $h_p$  is not a function of  $V_i$ ; but in the second case where  $V_i < V_{c,i}$ ,  $h_p$  is a function of  $V_i$ . In appendix C the partial derivative  $\frac{\partial(r_p/r_1)}{\partial(V_i/V_{c,i})}$  is evaluated at  $V_i = V_{c,i}$  and found to be

$$\frac{\partial(r_p/r_1)}{\partial(V_i/V_{c,i})} = 4 \quad (C47)$$

If equations (31) and (C47) are substituted into equation (26) two equations are obtained which are valid depending upon whether  $V_i > V_{c,i}$  or  $V_i < V_{c,i}$ . When these equations are modified to account for the physical effect of  $\Delta\gamma_1$  as was done for equation (23) they become

$$\Delta h_p = \Delta r_1 - \operatorname{sgn}(\Delta \gamma_1) r_1 \frac{\partial(r_p/r_1)}{\partial \gamma_1} \Delta \gamma_1 \quad \text{for } (V_1 + \Delta V_1) > V_{c,1} \quad (33a)$$

and

$$\Delta h_p = \Delta r_1 + 4 \frac{r_1}{V_{c,1}} \Delta V_1 - \operatorname{sgn}(\Delta \gamma_1) r_1 \frac{\partial(r_p/r_1)}{\partial \gamma_1} \Delta \gamma_1 \quad \text{for } (V_1 + \Delta V_1) < V_{c,1} \quad (33b)$$

When equations (20a), (20b), and (20c) are substituted into equations (33a) and (33b) and terms are combined one obtains

$$\Delta h_p = A'' \Delta V_0 + B'' \Delta \gamma_0 + C'' \Delta \omega + D'' \Delta \dot{\gamma}_1 + E'' \Delta \varphi \quad \text{for } ((V_1 + \Delta V_1) > V_{c,1}) \quad (34a)$$

and

$$\Delta h_p = F'' \Delta V_0 + G'' \Delta \gamma_0 + C'' \Delta \omega + D'' \Delta \dot{\gamma}_1 + E'' \Delta \varphi + H'' \Delta V_\delta \quad \text{for } ((V_1 + \Delta V_1) < V_{c,1}) \quad (34b)$$

where

$$A'' = A - \operatorname{sgn}(\Delta \gamma_1) r_1 \frac{\partial(r_p/r_1)}{\partial \gamma_1} E$$

$$B'' = B - \operatorname{sgn}(\Delta \gamma_1) r_1 \frac{\partial(r_p/r_1)}{\partial \gamma_1} F$$

$$C'' = -\operatorname{sgn}(\Delta \gamma_1) r_1 \frac{\partial(r_p/r_1)}{\partial \gamma_1} G$$

$$D'' = -\operatorname{sgn}(\Delta \gamma_1) r_1 \frac{\partial(r_p/r_1)}{\partial \gamma_1} H$$

$$E'' = -\operatorname{sgn}(\Delta \gamma_1) r_1 \frac{\partial(r_p/r_1)}{\partial \gamma_1} I$$

$$F'' = A + 4 \frac{r_1}{V_{c,1}} C - \operatorname{sgn}(\Delta \gamma_1) r_1 \frac{\partial(r_p/r_1)}{\partial \gamma_1} E$$

$$G'' = B + 4 \frac{r_1}{V_{c,1}} D - \operatorname{sgn}(\Delta \gamma_1) r_1 \frac{\partial(r_p/r_1)}{\partial \gamma_1} F$$

The expression  $\frac{\partial(r_p/r_1)}{\partial \gamma_1}$  is derived in appendix C (eq. (C44) and is presented in figure 12. Equations (34a) and (34b) are used to determine

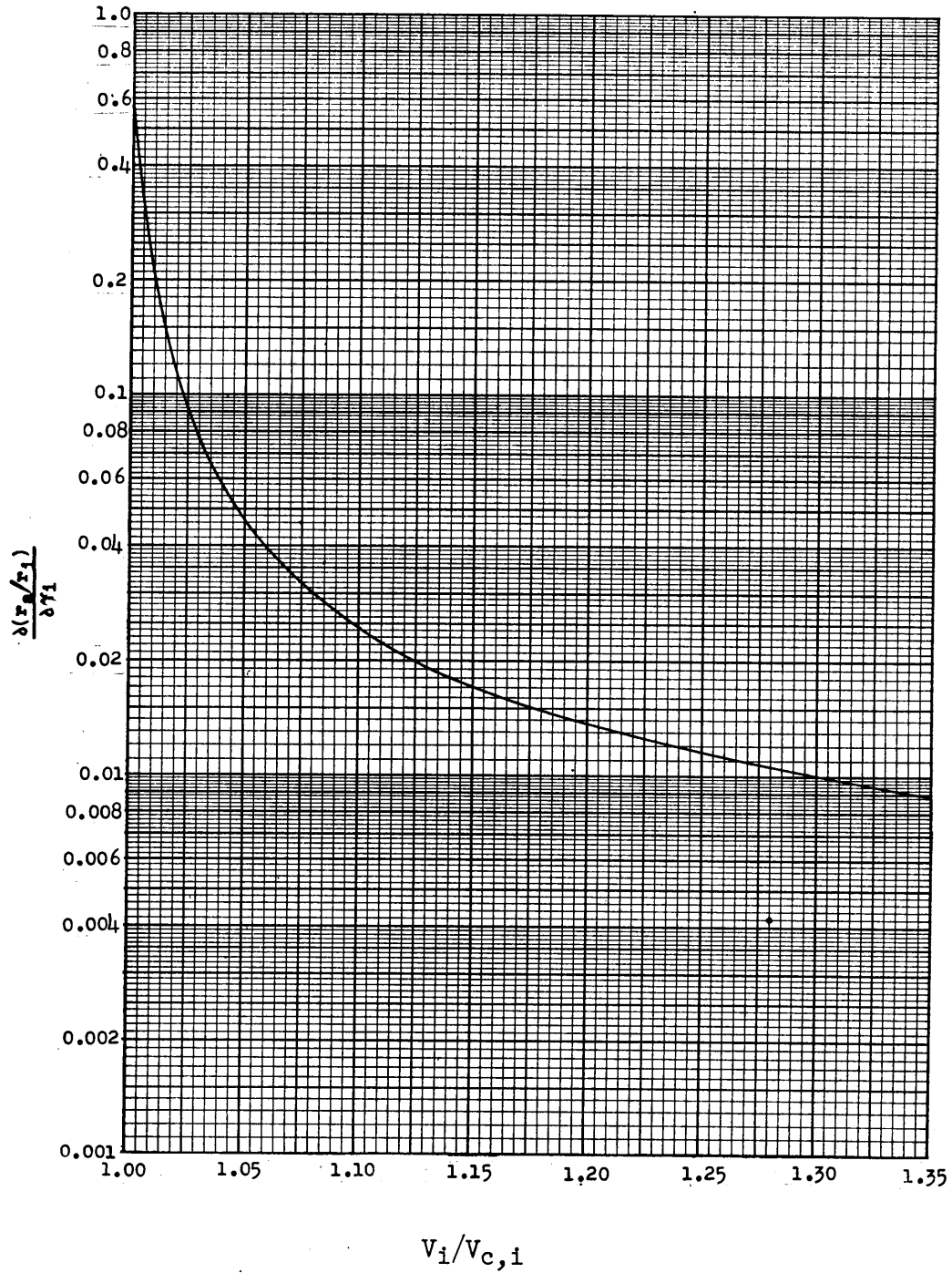


Figure 12.- Rate of change of  $r_a/r_1$  with respect to  $\gamma_1$  for values of  $V_i/V_{c,1}$ .

the standard deviation of the error in perigee altitude  $[\sigma(\Delta h_p)]$  as was done to determine  $[\sigma(\Delta h_a)]$ ; that is,

$$\sigma(\Delta h_p) = \left\{ (A'')^2 [\sigma(\Delta V_o)]^2 + (B'')^2 [\sigma(\Delta \gamma_o)]^2 + (C'')^2 [\sigma(\Delta \omega)]^2 + (D'')^2 [\sigma(\Delta \dot{\gamma}_1)]^2 + (E'')^2 [\sigma(\Delta \varphi)]^2 \right\}^{1/2} \text{ for } (V_i + \Delta V_i > V_{c,i}) \quad (35a)$$

and

$$\sigma(\Delta h_p) = \left\{ (F'')^2 [\sigma(\Delta V_o)]^2 + (G'')^2 [\sigma(\Delta \gamma_o)]^2 + (C'')^2 [\sigma(\Delta \omega)]^2 + (D'')^2 [\sigma(\Delta \dot{\gamma}_1)]^2 + (E'')^2 [\sigma(\Delta \varphi)]^2 + (H'')^2 [\sigma(\Delta V_\delta)]^2 \right\}^{1/2} \text{ for } (V_i + \Delta V_i < V_{c,i}) \quad (35b)$$

The range of validity of each of these equations is found by using the standard deviation of the injection velocity  $\sigma(\Delta V_i)$  as given in equation (21b).

If

$$\frac{V_i - V_{c,i}}{\sigma(\Delta V_i)} > -3$$

then equation (35a) is valid more than 99.7 percent of the time and may be considered to be valid over the entire range of  $\Delta h_p$ . When

$$\frac{V_i - V_{c,i}}{\sigma(\Delta V_i)} \leq -3$$

equations (35a) and (35b) are valid for some part of the range of  $\Delta h_p$ , however, the range of validity of each equation is not known. When

$$V_i = V_{c,i}$$

equation (35a) is valid for  $\Delta h_p > 0$  and equation (35b) is valid for  $\Delta h_p < 0$ . Since the range of validity of each equation is not known, the value of  $\sigma(\Delta h_p)$  given by equation (35a) will be used over the entire range. An indication of the effect of this obtained by comparing the value of  $\sigma(\Delta h_p)$  given by equation (35a) with that given by equation (35b).



### VIII. PROCEDURE FOR CALCULATING ERRORS

The purpose of this section is to present a detailed procedure for calculating the values of  $\sigma(\Delta r_1)$ ,  $\sigma(\Delta V_1)$ ,  $\sigma(\Delta \gamma_1)$ ,  $\sigma(\Delta h_a)$ , and  $\sigma(\Delta h_p)$  given by equations (21a), (21b), (21c), (25), (35a), and (35b). The parameters which affect the orbit with zero errors and which must be known are  $r_0$ ,  $V_0$ ,  $\gamma_0$ , and  $V_\delta$ . The type of trajectory considered here assumes that the last stage is ignited at the peak of the ascent trajectory and that the time of burning for the last stage is small. This results in the assumption that

$$\alpha_1 = \phi_1 = \gamma_1 = \gamma_i = 0$$

$$r_1 = r_i = (r_a)_{\text{ascent trajectory}}$$

$$V_1 = (V_a)_{\text{ascent trajectory}}$$

The value of  $r_1$  and  $V_1$  may be calculated using equations (A14) and (A21), respectively, where  $V_{c,0}$  is a function of  $r_0$  given by equation (A13) and  $e$  is a function of  $V_{c,0}$ ,  $V_0$ , and  $\gamma_0$  as given by equation (A15).

Since the angle of attack and attitude angle are equal to the flight-path angle during the burning of the last stage (all are equal to zero) the velocity increment ( $V_\delta$ ) is parallel to the velocity at ignition of the last stage ( $V_1$ ) and the injection velocity ( $V_i$ ) is

$$V_i = V_1 + V_\delta$$

The period of a circular orbit having a radius of  $r_0(T_{c,0})$  is given by equation (A26) and the circular velocity at a radius  $r_1(V_{c,1})$  is given by equation (A13).

It is also necessary to know the value of  $\sigma(\Delta V_0)$ ,  $\sigma(\Delta \gamma_0)$ ,  $\sigma(\Delta V_B)$ ,  $\sigma(\Delta \varphi)$ ,  $\sigma(\Delta \alpha)$ , and  $\sigma(\Delta \dot{\gamma}_1)$  which affect the errors in the trajectory.

The only quantities which still must be found are the partial derivatives appearing in equations (20a), (20b), (20c), (25), (34a), and (34b). The values of these partial derivatives are presented in figures 2 to 12. The partial derivatives, corresponding figure, and quantities which must be known are listed below.

| Partial derivatives                                   | Figure number | Quantities which must be known |
|---|---------------|--------------------------------|
| $\frac{\partial(r_1/r_0)}{\partial(v_0/v_{c,0})}$     | 2             | $v_0/v_{c,0}, \gamma_0$        |
| $\frac{\partial(r_1/r_0)}{\partial \gamma_0}$         | 3             | $v_0/v_{c,0}, \gamma_0$        |
| $\frac{\partial(v_1/v_{c,0})}{\partial(v_0/v_{c,0})}$ | 4             | $v_0/v_{c,0}, \gamma_0$        |
| $\frac{\partial(v_1/v_{c,0})}{\partial \gamma_0}$     | 5             | $v_0/v_{c,0}, \gamma_0$        |
| $\frac{\partial \theta}{\partial \gamma_0}$           | 6             | $v_0/v_{c,0}, \gamma_0$        |
| $\frac{\partial \theta}{\partial(v_0/v_{c,0})}$       | 7             | $v_0/v_{c,0}, \gamma_0$        |
| $\frac{\partial(t/T_{c,0})}{\partial \gamma_0}$       | 8             | $v_0/v_{c,0}, \gamma_0$        |
| $\frac{\partial(t/T_{c,0})}{\partial(v_0/v_{c,0})}$   | 9             | $v_0/v_{c,0}, \gamma_0$        |
| $\frac{\partial(r_a/r_i)}{\partial(v_1/v_{c,1})}$     | 10            | $v_1/v_{c,i}$                  |
| $\frac{\partial(r_a/r_i)}{\partial \gamma_1}$         | 11            | $v_1/v_{c,i}$                  |
| $\frac{\partial(r_p/r_i)}{\partial \gamma_1}$         | 12            | $v_1/v_{c,i}$                  |

The use of the figures (to determine the value of the partial derivatives) will greatly reduce the work required to obtain the final results.

The partial derivatives  $\frac{\partial \gamma_8}{\partial w}$  and  $\frac{\partial \gamma_8}{\partial \dot{\gamma}_1}$  can be found using the method of Buglia, Young, Timmons, and Brinkworth (ref. 6). It is necessary to know the mass, mass ratio, inertia, spin rate, and thrust characteristics of the last stage to use this method.

It is now possible to calculate  $\sigma(\Delta r_1)$ ,  $\sigma(\Delta V_1)$ ,  $\sigma(\Delta \gamma_1)$ ,  $\sigma(\Delta h_a)$ , and  $\sigma(\Delta h_p)$  using equations (21a), (21b), (21c), (26), (35a), and (35b). The value of  $\sigma(\Delta h_p)$  given by equation (35a) is used over the entire range of  $V_1 + \Delta V_1$ . The equations yield two values of  $\sigma(\Delta h_a)$  and  $\sigma(\Delta h_p)$ . The larger value of  $\sigma(\Delta h_a)$  corresponds to the case where  $\Delta h_a$  is positive while the larger value of  $\sigma(\Delta h_p)$  corresponds to the case where  $\Delta h_p$  is negative. Once the values of  $\sigma(\Delta r_1)$ ,  $\sigma(\Delta V_1)$ ,  $\sigma(\Delta \gamma_1)$ ,  $\sigma(\Delta h_a)$ , and  $\sigma(\Delta h_p)$  are known it is possible to determine the probability that  $r_1$ ,  $V_1$ ,  $\gamma_1$ ,  $h_a$ , and  $h_p$  will lie within a certain range of values.

### IX. ACCURACY OF PARTIAL DERIVATIVES

A series of 13 trajectories were calculated using an IBM 704 computer to determine the validity of the use of the partial derivatives. One trajectory was used as the nominal case and had the following initial conditions which are typical of those of the Scout.

$$h_0 = 687,251 \text{ feet}$$

$$x_0 = 570,427 \text{ feet}$$

$$V_0 = 19,565 \text{ feet per second}$$

$$\gamma_0 = 46.77^\circ$$

$$t_0 = 121 \text{ seconds}$$

The errors assumed in  $\gamma_0$  were  $-5^\circ$ ,  $-2^\circ$ ,  $+2^\circ$ , and  $+5^\circ$  and the errors in  $V_0$  were -3 percent, -1 percent, +1 percent, and +3 percent. These errors were combined to determine whether or not their effects could be added directly. These results are shown in table 1 where they are compared with the results of the present partial derivative method.

The values of  $\Delta V_A$ ,  $\Delta x_A$ ,  $\Delta r_A$ , and  $\Delta t_A$  indicate the validity of the assumption that the partial derivatives are linear over small ranges. The largest differences between the exact and approximate (linear method) values of these errors are less than 1.5 percent of the nominal values. The differences between the velocity and radius at the peak of the ascent trajectory and the velocity and radius at ignition of the last stage indicates the validity of the assumption used to derive  $\frac{\partial \gamma_1}{\partial t}$  and  $\frac{\partial \theta}{\partial t}$ . These assumptions were that  $V_1$  and  $r_1$  were constant near the peak of the ascent trajectory. The largest variation of  $V_1$  was 89 feet per

TABLE 1

|                            | 0        | 0        | 0        | 0        | -5 percent | -1 percent | +1 percent | +3 percent | -3 percent | -3 percent | -3 percent | +3 percent | +3 percent | +3 percent |
|----------------------------|----------|----------|----------|----------|------------|------------|------------|------------|------------|------------|------------|------------|------------|------------|
| $\Delta V_0$               | 0        | 0        | 0        | 0        | 0          | 0          | 0          | 0          | -2°        | -2°        | -2°        | +3°        | -2°        | +2 percent |
| $\Delta \theta_0$          | -5°      | -2°      | 2°       | 5°       | 0          | 0          | 0          | 0          | 0          | 0          | 0          | 0          | 0          | 0          |
| $\Delta V_A$ (approximate) | 1235     | 494      | -494     | -1235    | -114       | -38        | 38         | 114        | 380        | -608       | -608       | -608       | 608        | -380       |
| $\Delta V_A$ (exact)       | 1262     | 504      | -506     | -1261    | -120       | -34        | 33         | 92         | 374        | -613       | -613       | -613       | 608        | -422       |
| $\Delta V_A$ (approximate) | 547,810  | 219,214  | -219,124 | -547,810 | -615,763   | -205,604   | 205,604    | 615,263    | -396,639   | -834,887   | -834,887   | -834,887   | 834,887    | 396,639    |
| $\Delta V_A$ (exact)       | 506,746  | 224,133  | -250,143 | -660,322 | -585,347   | -203,138   | 198,619    | 613,976    | -396,181   | -802,408   | -802,408   | -802,408   | 874,728    | 334,798    |
| $\Delta V_A$ (approximate) | -709,440 | -283,636 | 283,636  | 709,440  | -511,864   | -170,912   | 170,912    | 511,864    | -795,500   | -228,228   | -228,228   | -228,228   | 228,228    | 795,500    |
| $\Delta V_A$ (exact)       | -729,327 | -286,754 | 278,215  | 680,516  | -519,898   | -179,443   | 185,754    | 572,744    | -786,175   | -261,606   | -261,606   | -261,606   | 265,298    | 871,310    |
| $\Delta V_A$ (approximate) | -51      | -20      | 20       | 51       | -69        | -23        | 27         | 69         | -89        | -49        | -49        | -49        | 49         | 89         |
| $\Delta V_A$ (exact)       | -50      | -18      | 19       | 43       | -58        | -20        | 21         | 64         | -76        | -40        | -40        | -40        | 44         | 82         |
| $V_A - V_1$                | -29      | -4       | 5        | 27       | 44         | 6          | -5         | -50        | -81        | -24        | -24        | -24        | -84        | -5         |
| $F_A - F_1$                | +17,306  | -2,426   | -2,571   | -14,155  | -24,563    | -3,302     | -2,768     | -28,954    | -44,436    | -12,452    | -12,452    | -12,452    | -14,071    | -48,215    |
| $\theta_1$ (approximate)   | -3.49    | -1.36    | 1.36     | 3.49     | -5.01      | -1.68      | 1.68       | 5.01       | -7.57      | -2.48      | -2.48      | -2.48      | 2.48       | 7.57       |
| $\theta_1$ (exact)         | -3.49    | -1.38    | 1.57     | 3.97     | -4.86      | -1.57      | 1.67       | 4.82       | -6.10      | -3.57      | -3.57      | -3.57      | 3.20       | 6.52       |

second ( $\approx 0.8$  percent of  $V_1$ ) and the largest variation of  $r_1$  was 28,954 feet ( $\approx 0.1$  percent of  $r_1$ ). This shows that the assumption was valid.

The largest disagreement between the exact and approximate values was for the flight-path angle at ignition of the last stage. Errors in this angle have the greatest effect upon the apogee and perigee altitudes of the final orbit. For the majority of cases, the difference between the exact and approximate values was less than  $0.25^\circ$ . Even the smallest error in this angle was approximately twice the maximum error expected for the Scout. The largest disagreement between the exact and approximate values occurred when the initial errors in  $V_0$  and  $\gamma_0$  were combined but the probability that both errors would be this large is very small ( $\ll 0.4$  percent). The approximate value of the flight-path angle at ignition of the last stage should be sufficiently accurate for the range of initial errors expected.

The approximate values calculated using the theory agree closely with the exact values obtained using the machine calculations. Comparison of the approximate and exact values indicate that the effects of different initial errors may be added directly to the same degree of accuracy as that obtained by using the partial derivatives.

### X. SAMPLE CALCULATIONS

The dispersion of the apogee and perigee altitudes were calculated for the Scout vehicle having the values of  $r_0$ ,  $V_0$ , and  $\gamma_0$  presented in figure 13. The values are functions of the peak altitude of the ascent trajectory ( $h_A$ ). The velocity increment of the last stage is 10,000 feet per second. The standard deviation of the primary errors are listed below.

| Error                   | Standard deviation ( $\sigma$ ) |
|-------------------------|---------------------------------|
| $\Delta V_0$            | 132 feet per second             |
| $\Delta \gamma_0$       | $0.50^\circ$                    |
| $\Delta V_B$            | 100 feet per second             |
| $\Delta \omega$         | $0.0333^\circ$                  |
| $\Delta \dot{\gamma}_1$ | $0.0666^\circ$ per second       |
| $\Delta \varphi$        | $0.333^\circ$                   |

These values do not correspond to those used in the previous section. The values of  $\sigma(\Delta V_0)$  and  $\sigma(\Delta \gamma_0)$  were determined by the method discussed in the section on general considerations. The quantities varied were the total impulse, initial weight, thrust alignment, and drag estimates of each stage; head or tail winds; and guidance accuracy. The effect of a "dead-band" region in the guidance system was included. The dead-band region is a small region around the reference position of the guidance system in which no control forces are applied in order to reduce the amount of fuel required by the hydrogen-peroxide rockets which comprise the reaction control system of the second and third stages.

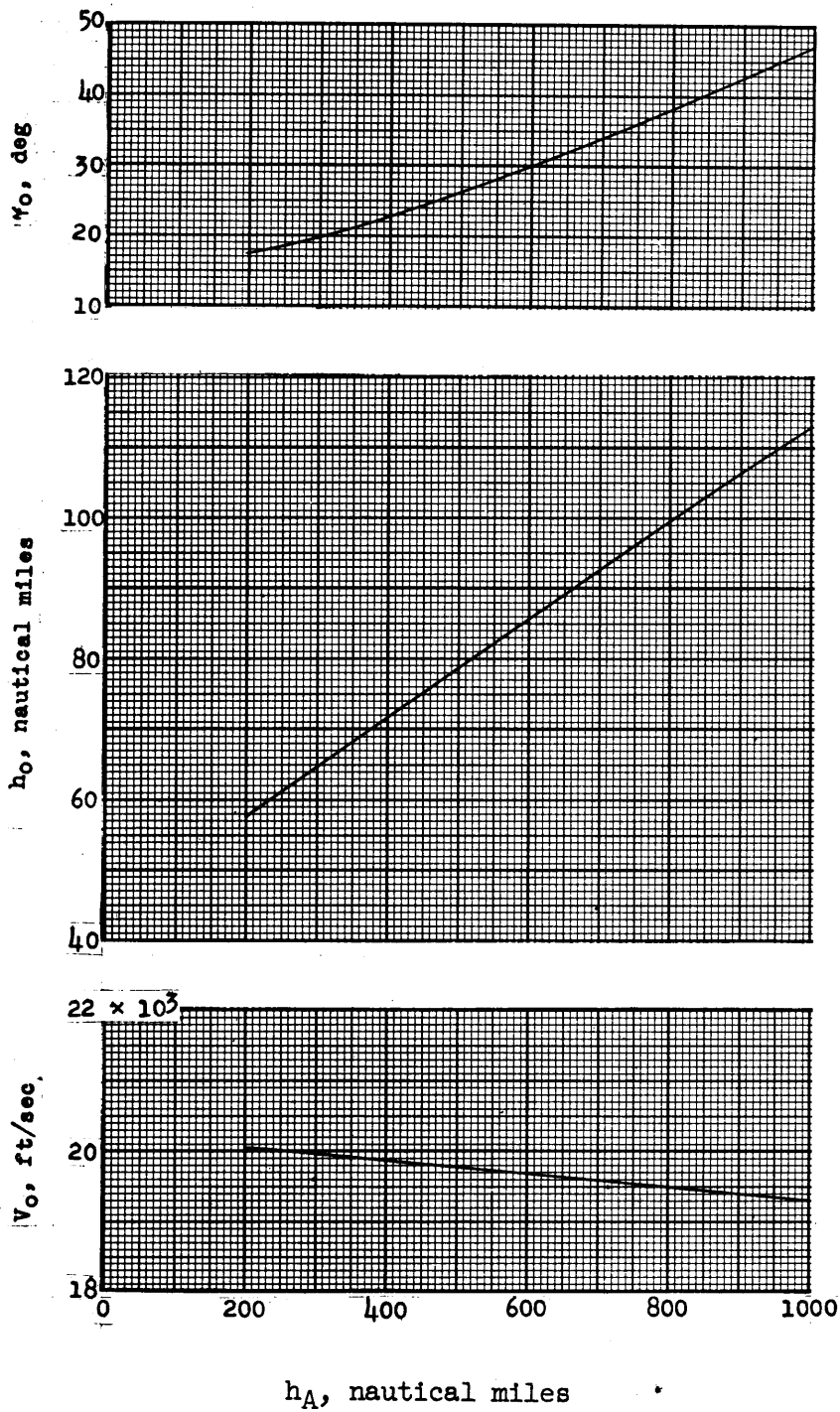


Figure 13.- Conditions at burnout of the next-to-the-last stage.



The magnitude of the standard deviation of the errors in the quantities determining the velocity and flight-path angle at the burnout of the next-to-last stage, and the standard deviations of  $\Delta V_8$ ,  $\Delta \omega$ ,  $\Delta \dot{\gamma}_1$ , and  $\Delta \varphi$  were those which were felt to be approximately the values obtainable in the Scout system.

Numerical values of the individual terms of equations (25) and (34a) are listed below for  $h_A = 200$  nautical miles. These values are typical of those at other values of  $h_A$  and indicate the relative size of the terms.

$$\begin{array}{rcccccc} \Delta h_a = A' \Delta V_0 + B' \Delta \gamma_0 + C' \Delta \omega + D' \Delta \dot{\gamma}_1 + E' \Delta \varphi + F' \Delta V_8 \\ 112.00 \quad 45.50 \quad 0.15 \quad 0.02 \quad 0.15 \quad 71.00 \end{array}$$

$$\begin{array}{rcccccc} \Delta h_p = A'' \Delta V_0 + B'' \Delta \gamma_0 + C'' \Delta \omega + D'' \Delta \dot{\gamma}_1 + E'' \Delta \varphi \\ 6.90 \quad 4.21 \quad 0.15 \quad 0.02 \quad 0.15 \end{array}$$

The dominant terms are those due to errors in  $V_0$ ,  $V_8$ , and  $\gamma_0$ . The remaining terms are at least one order of magnitude smaller than these terms and could be neglected in this case.

The results of the calculations are presented in figure 14. The lines designated 0 percent are the nominal values of  $h_a$  and  $h_p$ . The lines of equal value give the probability that  $h_a$  or  $h_p$  will lie within the range defined by the two lines. For example, at a  $h_A$  of 400 nautical miles, the probability that  $h_a$  will be between 2080 nautical miles and 2230 nautical miles is 50 percent. The largest dispersion in  $h_a$  occurs at the lower values of  $h_A$  while the dispersion in  $h_p$  is only slightly greater at the higher values of  $h_A$  than it is at the lower values of  $h_A$ .

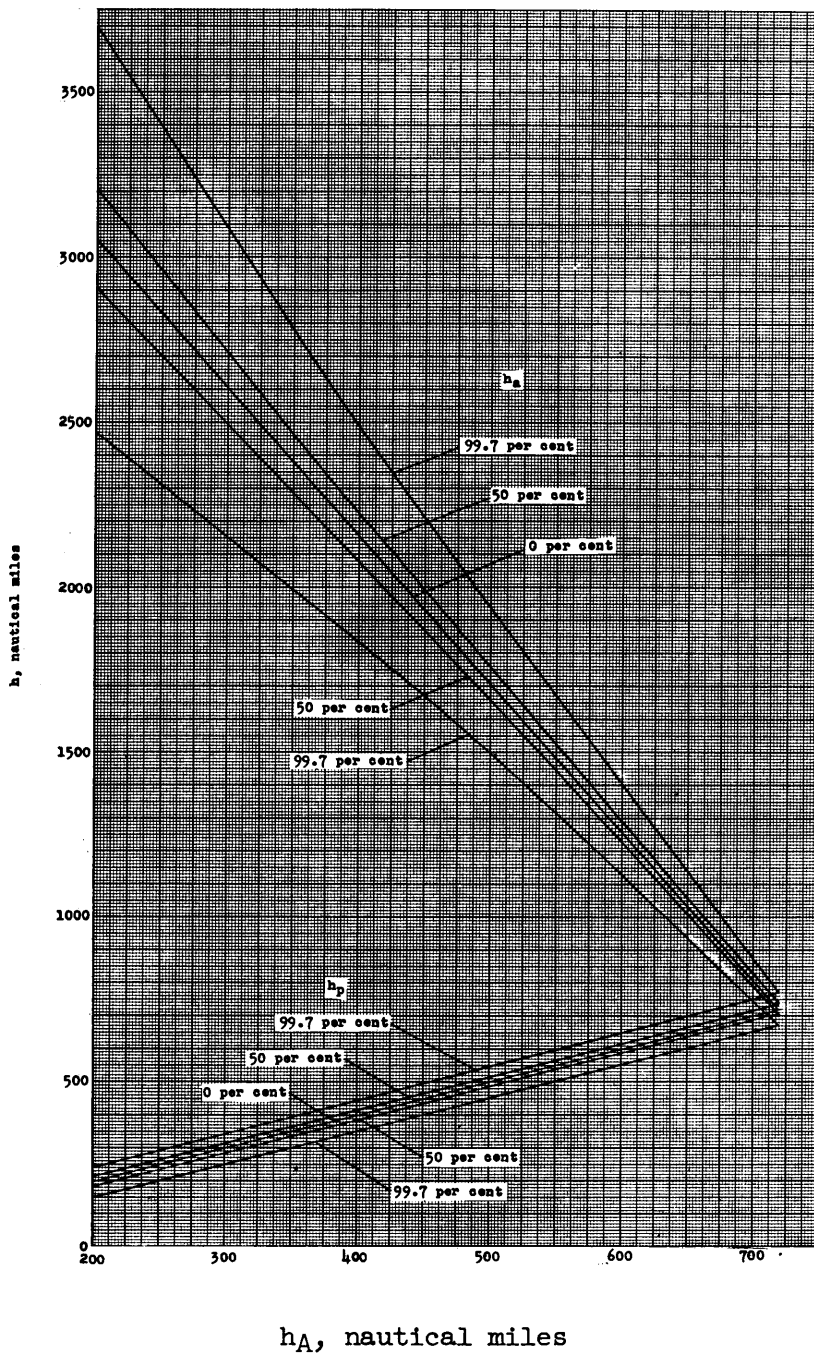


Figure 14.- Probable distribution of apogee and perigee altitudes of the Scout vehicle.

If the minimum permissible value of  $h_p$  is 200 nautical miles,  $h_A$  must be increased to 210 nautical miles before the probability is 50 percent that  $h_p$  will be greater than 200 nautical miles. If  $h_A$  is increased to 230 nautical miles, the probability that  $h_p$  will be greater than 200 nautical miles is 99.7 percent.

The theory considers that each component operates successfully within its individual tolerance and does not consider the probability that the components will not operate successfully. The importance of this statement may be realized by considering the preceding example. While the probability of  $h_p$  being greater than 200 nautical miles can be made very high ( $\gg$  99.7 percent) if everything operates successfully, it would be naive to believe that the Scout vehicle will be this reliable with no exceptions.

## XI. CONCLUSIONS

A theory has been developed which determines the influence of primary errors upon the dispersion of the apogee and perigee altitudes of the orbit of a satellite vehicle. It is seen that the apogee and perigee altitudes are influenced chiefly by the errors in velocity and flight-path angle at burnout of the next-to-last stage, guidance, velocity increment and thrust alignment, and pitching rate at ignition of the last stage. The theory will allow the probability of a satellite vehicle successfully obtaining a given orbit to be determined. A series of charts which greatly reduce the amount of work required in applying the theory are included.

The theory has been applied to the Scout missile for a range of injection altitudes and one payload weight which is representative of the capability of this vehicle. One of the major requirements of any future satellite vehicle will be an improved guidance system so that the Scout probably will be the worst case to which the theory will be applied.

## XII. ACKNOWLEDGMENTS

The author wishes to express his appreciation to the National Aeronautics and Space Administration for the opportunity to use material in this thesis which was obtained from an investigation conducted at their Langley Research Center.

He also wishes to thank Dr. Robert W. Truitt and Dr. James B. Eades of the Aeronautical Engineering Department of the Virginia Polytechnic Institute for their advice and assistance in preparing this thesis.

XIII. REFERENCES

1. The martin Company: Dynamic Analysis and Design Performance Requirements for Satellite Vehicle Guidance Systems. Engineering Report No. 10470-2 (Monthly Progress Report No. 2), The Martin Company (Baltimore), August 1958.
2. Gedeon, Geza S., and Dawley, Richard E.: The Influence of the Launching Conditions on the Orbital Characteristics. Jet Propulsion, vol. 28, no. 11, November 1958, pp. 759-760.
3. Benezra, Joseph N.: A Short Form Method for Determining Near-Circular Orbit Quantities. ARS Journal, vol. 24, no. 3, March 1959, pp. 217-219.
4. Sohn, Robert L.: Rapid Method for Computing High Altitude Gravity Turns. ARS Journal, vol. 29, no. 2, February 1959, pp. 140-142.
5. Meyler, Dorothy S., M. Sc., and Sutton, O. G., KT, CBE, D. Sc., F.R.S.: A Comperdium of Mathematics and Physics. D. Van Nostrand Company, Inc.
6. Buglia, James J., Young, George R., Timmons, Jesse D., and Brinkwood, Helen S.: Analytical Method of Approximating the Motion of a Spinning Vehicle With Variable Mass and Inertia Properties Acted Upon by Several Disturbing Parameters. Proposed NASA TN.
7. Hodgman, Charles O.: Standard Mathematical Tables. Chemical Rubber Publishing Company.
8. Margenau, H., and Murphy, G. M.: The Mathematics of Physics and Chemistry, p. 515; D. Van Nostrand Company, Inc., New York, 1949.

9. Goldstein, Herbert, Ph. D.: *Classical Mechanics*, Addison-Wesley  
Publishing Company, Inc.
10. Ramsey, A.S., M.A.: *Dynamics, Part II*. Cambridge University Press.

**The vita has been removed from  
the scanned document**



XV. APPENDICES

APPENDIX A. Development of the Ballistic Equations

in the Forms Used

The equation of the orbit is given by Goldstein (ref. 9) as

$$\frac{1}{r} = \frac{mk}{L^2} [1 + e \cos (\theta - \theta')] \quad (A1)$$

where

$$k = m\mu \quad (A2)$$

$$L = mr^2\dot{\theta} = mr V \cos \gamma \quad (A3)$$

$\theta'$  = constant of integration

The eccentricity ( $e$ ) is

$$e = \left[ 1 + \frac{2EL^2}{mk^2} \right]^{1/2} \quad (A4)$$

and the total energy ( $E$ ) is

$$E = \frac{mv^2}{2} - \frac{k}{r} \quad (A5)$$

The eccentricity may be rewritten in the form

$$e = \left\{ 1 + \frac{r^2 v^2}{\mu} \left[ v^2 - 2 \frac{\mu}{r} \right] \cos^2 \gamma \right\}^{1/2} \quad (A6)$$

Usual convention is to measure the central angle from the line joining the focus and the perigee, but for convenience the central angle will be measured here from the line connecting the focus and the apogee so that the constant of integration ( $\theta'$ ) is zero. After substitution of

equations (A2) and (A3) into equation (A1) and rearrangement, equation (A1) becomes

$$r = \frac{(r_j V_j \cos \gamma)^2}{\mu(1 - e \cos \theta_j)} \quad (A7)$$

The subscript  $j$  refers to any general condition and is used for simplicity. The apogee ( $\theta_j = 0$ ) and the perigee ( $\theta_j = \pi$ ) radii are, respectively,

$$r_a = \frac{(r_j V_j \cos \gamma_j)^2}{\mu(1 - e)} \quad (A8)$$

and

$$r_p = \frac{(r_j V_j \cos \gamma_j)^2}{\mu(1 + e)} \quad (A9)$$

The injection radius is the radius at ignition of the last stage (assumed to be equal to the apogee radius of the ascent trajectory) plus the change in radius during the burning of the last stage ( $r_\delta$ )

$$r_i = \frac{r_o^2 V_o^2 \cos^2 \gamma_o}{\mu(1 - e)} + r_\delta \quad (A10)$$

where  $r_o$ ,  $V_o$ , and  $\gamma_o$  are the conditions at the burnout of the next-to-last stage.

The apogee and perigee altitudes, based on injection conditions, are respectively

$$h_a = \frac{r_i^2 V_i^2 \cos^2 \gamma_i}{\mu(1 - e)} - R \quad (A11)$$

and

$$h_p = \frac{r_i^2 V_i^2 \cos^2 \gamma_i}{\mu(1 + e)} - R \quad (A12)$$

since

$$h = r - R \quad (A13)$$

Since the velocity necessary to achieve a circular orbit at a given radius is

$$v_{c,j}^2 = \frac{\mu}{r_j}$$

the equations for  $r_1$ ,  $h_a$ , and  $h_p$  may be simplified by the use of this relation to give

$$\frac{r_1}{r_0} = \left( \frac{v_0}{v_{c,0}} \right)^2 \frac{\cos^2 \gamma_0}{1 - e} \quad (A14)$$

where

$$e = \left\{ 1 + \left( \frac{v_0}{v_{c,0}} \right)^2 \left[ \left( \frac{v_0}{v_{c,0}} \right)^2 - 2 \right] \cos^2 \gamma_0 \right\}^{1/2} \quad (A15)$$

$$h_a = \left( \frac{v_1}{v_{c,1}} \right)^2 \frac{\cos^2 \gamma_1}{1 - e} r_1 - R \quad (A16)$$

and

$$h_p = \left( \frac{v_1}{v_{c,1}} \right)^2 \frac{\cos^2 \gamma_1}{1 + e} r_1 - R \quad (A17)$$

where

$$e = \left\{ 1 + \left( \frac{v_1}{v_{c,1}} \right)^2 \left[ \left( \frac{v_1}{v_{c,1}} \right)^2 - 2 \right] \cos^2 \gamma_1 \right\}^{1/2} \quad (A18)$$

In a central force field, the angular momentum ( $L$ ) is conserved.

If the angular momentum at the burnout of the next-to-last stage and that at ignition of the last stage (apogee of the ascent trajectory) are equated the resulting equation is

$$r_1 v_1 = r_0 v_0 \cos \gamma_0 \quad (A19)$$

or

$$\frac{v_1}{v_0} = \frac{r_0}{r_1} \cos \gamma_0 \quad (\text{A20})$$

After substitution of equation (A14), and rearrangement, equation (A20) becomes

$$\left( \frac{v_1}{v_{c,0}} \right) = \frac{1}{\cos \gamma_0} \left( \frac{v_{c,0}}{v_0} \right) (1 - e) \quad (\text{A21})$$

The central angle, between the point of the burnout of the next-to-last stage and the apogee of the ascent trajectory, is found by solving equation (A7) for  $\theta$  and substituting from equation (A13) to obtain

$$\theta = \cos^{-1} \left\{ \frac{1}{e} \left[ 1 - \left( \frac{r_0}{r} \right) \left( \frac{v_0}{v_{c,0}} \right)^2 \cos^2 \gamma_0 \right] \right\} \quad (\text{A22})$$

Now setting  $r = r_0$ , then

$$\theta = \cos^{-1} \left\{ \frac{1}{e} \left[ 1 - \left( \frac{v_0}{v_{c,0}} \right)^2 \cos^2 \gamma_0 \right] \right\} \quad (\text{A23})$$

The time required to travel from the perigee to any point on an elliptical orbit is given by Ramsey (ref. 10) as

$$t' = \frac{a^{3/2}}{\sqrt{\mu}} 2 \left\{ \tan^{-1} \left[ \sqrt{\frac{1-e}{1+e}} \tan \frac{\theta_j}{2} \right] - \frac{e \sqrt{1-e^2} \sin \theta_j}{1+e \cos \theta_j} \right\} \quad (\text{A24})$$

The period of the orbit will be twice the time required to travel from the perigee to the apogee ( $\theta_j = \pi$ ), or,

$$T = \frac{2\pi a^{3/2}}{\sqrt{\mu}} \quad (\text{A25})$$

Hence the period of a circular orbit of radius  $r_j$  is

$$T_{c,j} = \frac{2\pi r_j^{3/2}}{\sqrt{\mu}} \quad (\text{A26})$$

The time required to travel from the point to apogee ( $t$ ) is one half the period minus the time required to travel from the perigee to the point. Thus the central angle is redefined as

$$\theta'_j = \pi - \theta_j$$

so that

$$t = \frac{\pi a^{3/2}}{\sqrt{\mu}} \left\{ 1 - \frac{\sqrt{1-e^2}}{\pi} \left[ \frac{2}{\sqrt{1-e^2}} \tan^{-1} \left( \sqrt{\frac{1-e}{1+e}} \tan \frac{\pi - \theta_j}{2} \right) - \frac{e \sin \theta_j}{1 - e \cos \theta_j} \right] \right\} \quad (\text{A27})$$

This equation may be written in a nondimensional form on dividing by the period of a circular orbit; that is,

$$\frac{t}{T_{c,j}} = \frac{1}{2} \left( \frac{a}{r_j} \right)^{3/2} \left\{ 1 - \frac{\sqrt{1-e^2}}{\pi} \left[ \frac{2}{\sqrt{1-e^2}} \tan^{-1} \left( \sqrt{\frac{1-e}{1+e}} \tan \frac{\pi - \theta_j}{2} \right) - \frac{e \sin \theta_j}{1 - e \cos \theta_j} \right] \right\} \quad (\text{A28})$$

Since the semi-major axis ( $a$ ) can be expressed as

$$a = \frac{l_j}{1 - e^2} \quad (\text{A29})$$

where

$$l_j = \frac{r_j^2 v_j^2 \cos^2 \gamma_j}{\mu}$$

or

$$l_j = r_j \left( \frac{v_j}{v_{c,j}} \right)^2 \cos^2 \gamma_j \quad (\text{A30})$$

then

$$\frac{a}{r_j} = \left( \frac{V_j}{V_{c,j}} \right)^2 \frac{\cos^2 \gamma_j}{1 - e^2} \quad (\text{A31})$$

If equation (A31) is substituted into equation (A32), and referenced to conditions at burnout of the next-to-last stage, the nondimensional time equation becomes

$$\frac{t}{T_{c,0}} = \frac{1}{2} \left( \frac{V_0}{V_{c,0}} \right)^3 \frac{\cos^3 \gamma_0}{(1 - e^2)^{3/2}} \left\{ 1 - \frac{\sqrt{1 - e^2}}{\pi} \left[ \frac{2}{\sqrt{1 - e^2}} \tan^{-1} \left( \sqrt{\frac{1 - e}{1 + e}} \tan \frac{\pi - \theta}{2} \right) - \frac{e \sin \theta}{1 - e \cos \theta} \right] \right\} \quad (\text{A32})$$

The injection velocity is related to  $V_1$ ,  $\varphi$ , and  $V_8$ , as shown by figure 15, as

$$V_1 = \left\{ (V_1 + V_8 \cos \varphi)^2 + (V_8 \sin \varphi)^2 \right\}^{1/2} \quad (\text{A33})$$

where  $V_1$  is a function of  $r_0$ ,  $V_0$ , and  $\gamma_0$ . This may be seen by referring to equations (A13), (A14), (A15), and (A21). These equations may be compared to give  $V_1$  as a function of  $r_0$ ,  $V_0$ , and  $\gamma_0$  only.

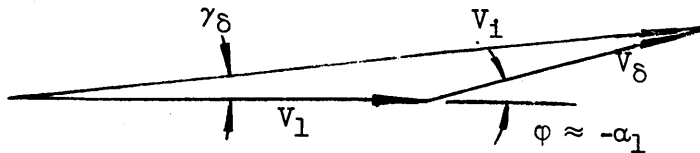


Figure 15.- Addition of velocity vectors.

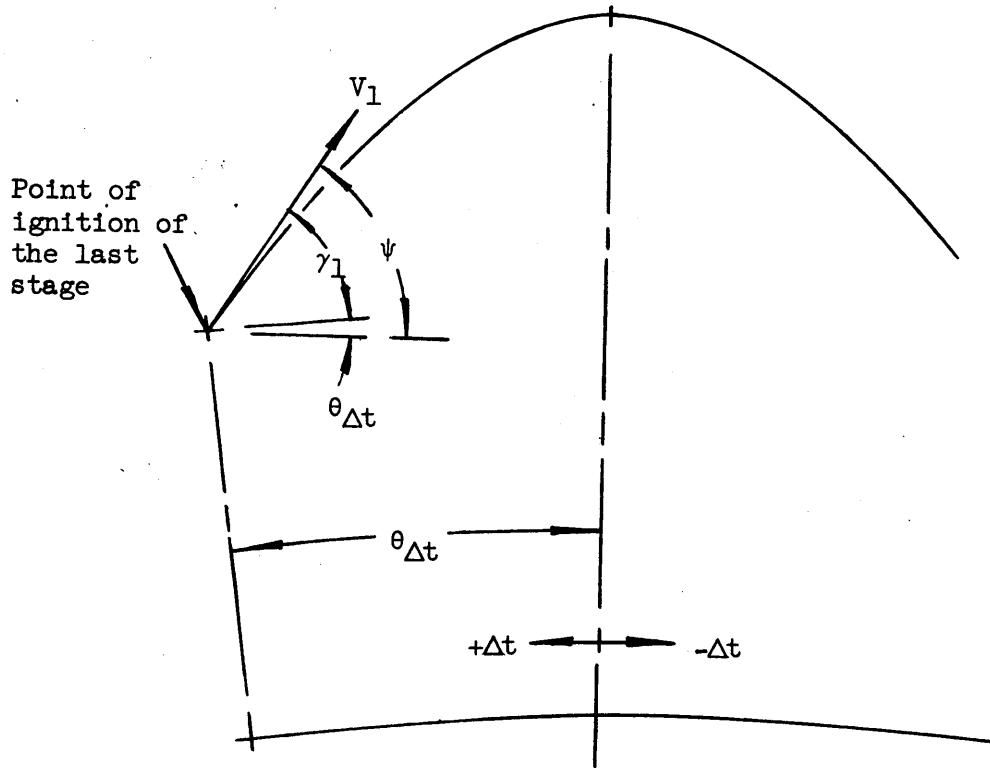


Figure 16.- Relationship of  $\gamma_1$ , to  $\psi$  and  $\theta_{\Delta t}$ .

APPENDIX B. Development of the Equation for the  
Error in Injection Angle

The basic equation for the error in the injection angle is given by equation (19) as

$$\Delta\gamma_1 = \Delta\gamma_1 + \Delta\gamma_8 + \Delta\gamma_p + \Delta\gamma_8 \quad (19)$$

The error in the flight-path angle at ignition of the last stage ( $\Delta\gamma_1$ ) results from the error in the time required to reach the peak of the ascent trajectory ( $\Delta t$ ). This relation is shown in figure 16. The figure shows that

$$\gamma = \psi - \theta_{\Delta t} \quad (B2)$$

where

$\psi$  is the angle between the tangent to the flight-path at the ignition of the last stage and the local horizontal at the peak of the elliptic trajectory followed by the vehicle during the coast period; and  $\theta_{\Delta t}$  is the central angle between the point of ignition of the last stage and the peak of the elliptic trajectory (followed by the vehicle during the coast period).

The error in  $\gamma_1$  is

$$\Delta\gamma_1 = \Delta\psi - \Delta\theta_{\Delta t} \quad (B2)$$

The error in time ( $\Delta t$ ) is defined as the total time required to reach the peak of the actual ascent trajectory minus the total time required to reach the peak of the ascent trajectory with no errors. The time of ignition of the last stage is assumed to be equal to the time at which the peak of the ascent trajectory with no errors would be reached. It is also assumed that the errors in the times of burnout of the next-to-



last stage and the ignition of the last stage are negligible. A positive value of  $\Delta t$  means that time required to reach the peak of the actual trajectory is increased or that the last stage is ignited before the peak is reached. The magnitude of the errors in  $\psi$  and  $\theta_{\Delta t}$  may be expressed as a function of  $\frac{\partial \psi}{\partial t}$ ,  $\frac{\partial \theta_{\Delta t}}{\partial t}$  and  $\Delta t$  where  $\frac{\partial \psi}{\partial t}$  and  $\frac{\partial \theta_{\Delta t}}{\partial t}$  are estimated from the curvature of the ascent ellipse and are derived in appendix C (eqs. (C39) and (C40)). The direction of the errors may be determined from figure 16. Since the final values of  $\psi$  and  $\theta_{\Delta t}$  are zero for a perfect injection, the errors are identically equal to  $\psi$  and  $\theta_{\Delta t}$  along the actual trajectory at some point other than the peak. Thus  $\psi$  and  $\theta_{\Delta t}$ , or  $\Delta\psi$  and  $\Delta\theta_{\Delta t}$  may be expressed by the following relation

$$\Delta\psi = - \frac{\partial \psi}{\partial t} \Delta t \quad (B3)$$

and

$$\Delta\theta_{\Delta t} = \frac{\partial \theta}{\partial t} \Delta t \quad (B4)$$

or

$$\Delta\gamma_1 = - \left( \frac{\partial \psi}{\partial t} + \frac{\partial \theta_{\Delta t}}{\partial t} \right) \Delta t \quad (B5)$$

Substituting  $\frac{\partial \psi}{\partial t}$  and  $\frac{\partial \theta_{\Delta t}}{\partial t}$  from equations (C39) and (C40) into

equation (B5) yields

$$\Delta\gamma_1 = \frac{v_1}{r_1} \left( \frac{e}{1-e} \right) \Delta t \quad (B6)$$

where  $V_1$  is determined from equation (A21),  $r_1$  from equation (A14),  $e$  from equation (A15), and  $\Delta t$  from equation (B13).

The change in flight-path angle during the burning of the last stage will be

$$\gamma_8 = \tan^{-1} \frac{V_8 \sin \alpha_1}{V_1 + V_8 \cos \alpha_1} \quad (B7)$$

as is shown by figure 15 if the time of burning is assumed to be small. The burning of the last stage occurs close to the peak of the ascent trajectory so that

$$\alpha \approx -\varphi$$

This approximation explains the apparent discrepancy between figures 1 and 16.

The error in  $\gamma_8$  is

$$\Delta\gamma_8 = \frac{\partial\gamma_8}{\partial V_8} \Delta V_8 + \frac{\partial\gamma_8}{\partial V_1} \Delta V_1 + \frac{\partial\gamma_8}{\partial \alpha_1} \Delta \alpha_1 \quad (B8)$$

where the partial derivative  $\frac{\partial\gamma_8}{\partial V_8}$ ,  $\frac{\partial\gamma_8}{\partial V_1}$ ,  $\frac{\partial\gamma_8}{\partial \alpha_1}$  are derived in appendix C (eqs. (C21), (C22), and (C23)).

The angle of attack at ignition of the last stage ( $\alpha_1$ ) is dependent upon the attitude (referenced to the local horizontal at the peak of the ascent trajectory with no errors) maintained by the guidance ( $\varphi$ ), the angle between the flight path at ignition and the local horizontal at the peak of the actual ascent trajectory ( $\psi$ ), and the central angle between the peak of the actual ascent trajectory and the peak of the ascent trajectory with no errors ( $\Delta\theta$ ). This relationship is shown in figure 17 to be

$$-\alpha_1 = \psi + (-\Delta\theta) - \varphi \quad (B9)$$

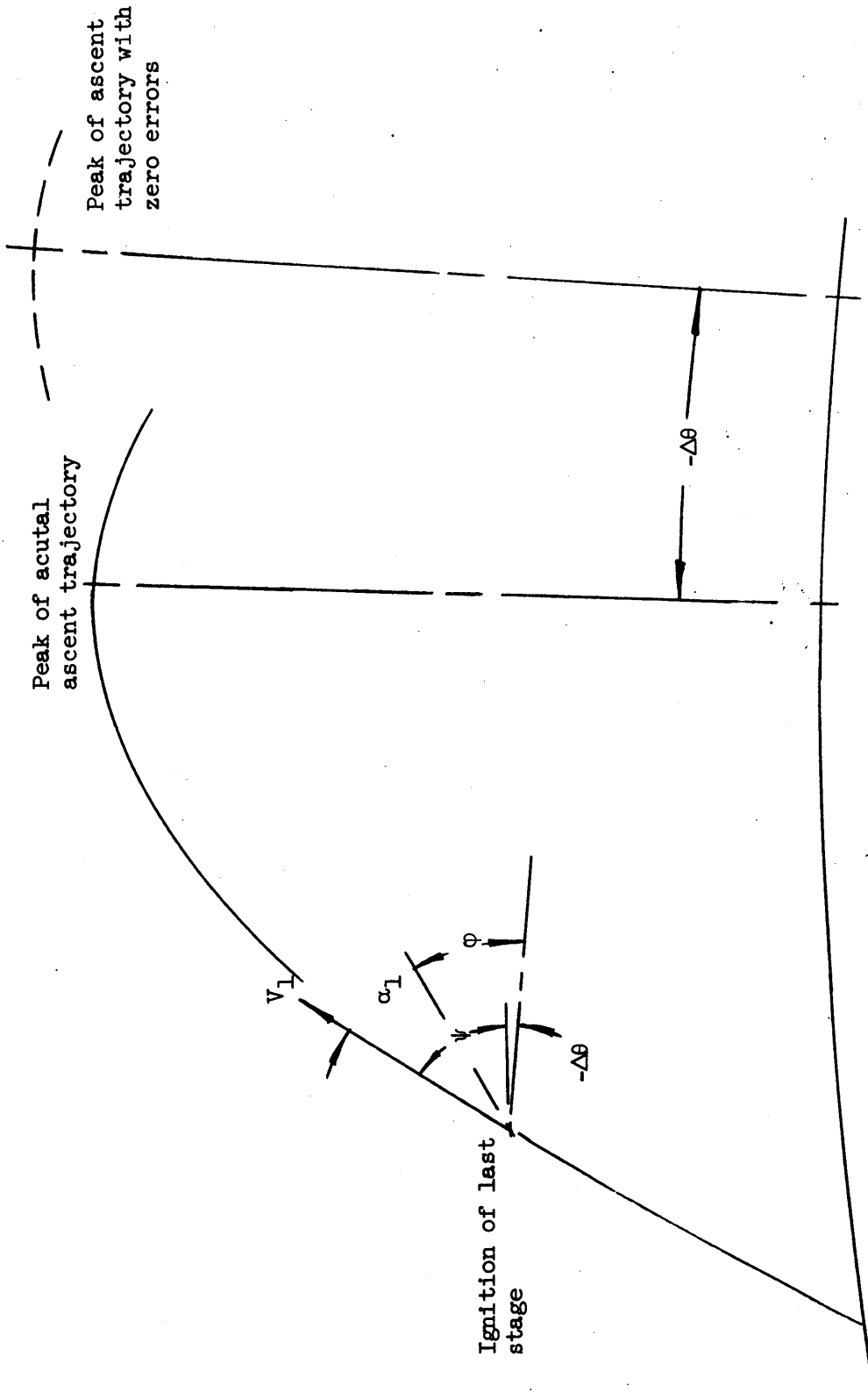


Figure 17.- Relation of angles influencing the angle of attack at ignition of the last stage.

and thus the error in the angle of attack is

$$\Delta\alpha_1 = \Delta\varphi - \Delta\psi + \Delta\theta \quad (\text{B10})$$

When equation (B3) is substituted into this expression, then

$$\Delta\alpha_1 = \Delta\varphi + \frac{\partial\psi}{\partial t} \Delta t + \Delta\theta \quad (\text{B11})$$

The central angle between the burnout of the next-to-last stage and the peak of the ascent trajectory with no errors is a function of the following quantities (eq. (A23)):

$$\theta = f(\gamma_0, V_0, r_0)$$

and therefore the error in  $\theta$  is

$$\Delta\theta = \frac{\partial\theta}{\partial\gamma_0} \Delta\gamma_0 + \frac{1}{V_{c,0}} \frac{\partial\theta}{\partial(V_0/V_{c,0})} \Delta V_0 \quad (\text{B12})$$

since  $r_0$  is assumed constant and fixes the value of  $V_{c,0}$ . The partial derivatives,  $\frac{\partial\theta}{\partial\gamma_0}$  and  $\frac{\partial\theta}{\partial(V_0/V_{c,0})}$ , are derived in appendix C (eqs. (C5) and (C6)) and are presented in figures 6 and 7.

The time required to travel from the burnout of the next-to-last stage to the peak of the ascent trajectory with no errors is a function of the following quantities (eq. (A32)):

$$t = f(r_0, V_0, \gamma_0)$$

Thus the error in time is expressed as

$$\Delta t = T_{c,0} \frac{\partial(t/T_{c,0})}{\partial\gamma_0} \Delta\gamma_0 + \frac{T_{c,0}}{V_{c,0}} \frac{\partial(t/T_{c,0})}{\partial(V_0/V_{c,0})} \Delta V_0 \quad (\text{B13})$$

since  $r_0$  is assumed constant and fixes the values of  $T_{c,0}$  and  $V_{c,0}$ .

The partial derivatives  $\frac{\partial(t/T_{c,0})}{\partial\gamma_0}$  and  $\frac{\partial(t/T_{c,0})}{\partial(V_0/V_{c,0})}$  are derived in appendix C (eqs. (C7) and (C8)) and presented in figures 8 and 9.

The change in the flight-path angle due to disturbances of the spinning last stage may be expressed as

$$\Delta\gamma_8 = \frac{\partial\gamma_8}{\partial\omega} \Delta\omega + \frac{\partial\gamma_8}{\partial\dot{\gamma}_1} \Delta\dot{\gamma}_1 \quad (B14)$$

Buglia, Young, Timmons, and Brinkworth (ref. 6) have presented a method for calculating the value of  $\gamma_8$  as a function of  $\omega$  and  $\dot{\gamma}_1$ . This information is used to find the value of  $\frac{\partial\gamma_8}{\partial\omega}$  and  $\frac{\partial\gamma_8}{\partial\dot{\gamma}_1}$ . These partial derivatives are functions of the moments of inertia, mass, motor performance, spin rate, etc., of the last stage.

The thrusting of the last stage takes place at a sufficiently great altitude that there is essentially no drag. The effect of gravity upon the velocity increment is negligible since the flight-path angle is almost zero. Therefore the central angle traveled during the burning of the last stage is a function of the velocity at ignition of the last stage ( $V_1$ ) and the velocity increment of the last stage ( $V_8$ ), or,

$$\theta_8 = f(V_1, V_8)$$

Then the error in  $\theta_8$  is expressed as

$$\Delta\theta_8 = \frac{\partial\theta_8}{\partial V_1} \Delta V_1 + \frac{\partial\theta_8}{\partial V_8} \Delta V_8 \quad (B15)$$

or

$$\Delta\theta_8 = \frac{\partial\theta_8}{\partial v_1} \left[ \frac{\partial(v_1/v_{c,o})}{\partial(v_o/v_{c,o})} \Delta v_o + v_{c,o} \frac{\partial(v_1/v_{c,o})}{\partial\gamma_o} \Delta\gamma_o \right] + \frac{\partial\theta_8}{\partial v_8} \Delta v_8 \quad (B16)$$

The partial derivatives  $\frac{\partial\theta_8}{\partial v_8}$  and  $\frac{\partial\theta_8}{\partial v_1}$  are given in appendix C (eqs. (C28) and (C29)).

When equations (18), (B5), (B8), (B11), (B12), (B13), (B14), and (B16) are combined they yield

$$\begin{aligned} \Delta\gamma_1 = & \left\{ \frac{T_{c,o}}{v_{c,o}} \left[ \frac{\partial\psi}{\partial t} \left( \frac{\partial\gamma_8}{\partial\alpha} - 1 \right) - \frac{\partial\theta_{\Delta t}}{\partial t} \right] \frac{\partial(t/T_{c,o})}{\partial(v_o/v_{c,o})} + \frac{\partial\gamma_8}{\partial v_1} \frac{\partial(v_1/v_{c,o})}{\partial(v_o/v_{c,o})} + \right. \\ & \left. \frac{1}{v_{c,o}} \frac{\partial\gamma_8}{\partial\alpha_1} \frac{\partial\theta_o}{\partial(v_o/v_{c,o})} + \frac{\partial\theta_8}{\partial v_1} \frac{\partial(v_1/v_{c,o})}{\partial(v_o/v_{c,o})} \right\} \Delta v_o + \left\{ T_{c,o} \left[ \frac{\partial\psi}{\partial t} \left( \frac{\partial\gamma_8}{\partial\alpha} - 1 \right) - \right. \right. \\ & \left. \left. \frac{\partial\theta_{\Delta t}}{\partial t} \right] \frac{\partial(t/T_{c,o})}{\partial\gamma_o} + v_{c,o} \frac{\partial\gamma_8}{\partial v_1} \frac{\partial(v_1/v_{c,o})}{\partial\gamma_o} + \frac{\partial\gamma_8}{\partial\alpha_1} \frac{\partial\theta_o}{\partial\gamma_o} + v_{c,o} \frac{\partial\theta_8}{\partial v_1} \frac{\partial(v_1/v_{c,o})}{\partial\gamma_o} \right\} \times \\ & \Delta\gamma_o + \left( \frac{\partial\gamma_8}{\partial v} + \frac{\partial\theta_8}{\partial v} \right) \Delta v_8 + \frac{\partial\gamma_8}{\partial\alpha} \Delta\varphi + \frac{\partial\gamma_8}{\partial\omega} \Delta\omega + \frac{\partial\gamma_8}{\partial\dot{\gamma}_1} \Delta\dot{\gamma}_1 \quad (B17) \end{aligned}$$

Now the equations for the partial derivatives  $\frac{\partial\gamma_8}{\partial v_8}$ , (C21);  $\frac{\partial\gamma_8}{\partial v_1}$ , (C22);

$\frac{\partial\gamma_8}{\partial\alpha_1}$ , (C23);  $\frac{\partial\theta_8}{\partial v_8}$ , (C28);  $\frac{\partial\theta_8}{\partial v_1}$ , (C29);  $\frac{\partial\psi}{\partial t}$ , (C39); and  $\frac{\partial\theta_{\Delta t}}{\partial t}$ , (C40) are

substituted into equation (B17) yielding

$$\begin{aligned}
 \Delta\gamma_1 = & \left\{ \frac{T_{c,o}}{V_{c,o}} \frac{1}{1-e} \left[ e - \frac{v_\delta}{v_1} \right] \frac{v_1}{r_1} \frac{\partial(t/T_{c,o})}{\partial(v_o/v_{c,o})} - \frac{1}{v_\delta} \left( \frac{v_\delta}{v_1} \right)^2 \frac{\partial\theta_o}{\partial\gamma_o} \frac{\partial(v_1/v_{c,o})}{\partial(v_o/v_{c,o})} \Delta\gamma_o + \right. \\
 & \left. \frac{1}{v_{c,o}} \frac{v_\delta}{v_1} \frac{\partial\theta}{\partial(v_o/v_{c,o})} + \frac{t_\delta}{r_1} \frac{\partial(v_1/v_{c,o})}{\partial(v_o/v_{c,o})} \right\} \Delta V_o + \left\{ T_{c,o} \frac{1}{1-e} \left[ e - \frac{v_\delta}{v_1} \right] \frac{v_1}{r_1} \frac{\partial(t/T_{c,o})}{\partial\gamma_o} - \right. \\
 & \left. \frac{v_{c,o}}{v_\delta} \left( \frac{v_\delta}{v_1} \right)^2 \frac{\partial\theta_o}{\partial\gamma_o} \frac{\partial(v_1/v_{c,o})}{\partial\gamma_o} \Delta\gamma_o + \frac{v_\delta}{v_1} \frac{\partial\theta_o}{\partial\gamma_o} + v_{c,o} \frac{t_\delta}{r_1} \frac{\partial(v_1/v_{c,o})}{\partial\gamma_o} \right\} \Delta\gamma_o + \\
 & \left\{ \frac{1}{v_1} \left( \frac{v_1}{v_1} \right)^2 \frac{\partial\theta_o}{\partial\gamma_o} \Delta\gamma_o + \frac{v_e t_\delta}{r_1} \frac{1 - (w_1/w_1) + \ln(w_1/w_1)}{[1 - (w_1/w_1)]^2} \right\} \Delta V_\delta + \frac{v_\delta}{v_1} \Delta\varphi + \\
 & \frac{\partial\gamma_\delta}{\partial\omega} \Delta\omega + \frac{\partial\gamma_\delta}{\partial\dot{\gamma}_1} \Delta\dot{\gamma}_1
 \end{aligned} \tag{B18}$$

If the individual terms are evaluated over the range of interest for the Scout, it is found that the following terms are small compared to the others:

$$\begin{aligned}
 & \frac{1}{v_\delta} \left( \frac{v_\delta}{v_1} \right)^2 \frac{\partial\theta_o}{\partial\gamma_o} \frac{\partial(v_1/v_{c,o})}{\partial(v_o/v_{c,o})} \Delta\gamma_o \Delta V_o; \quad \frac{t_\delta}{r_1} \frac{\partial(v_1/v_{c,o})}{\partial(v_o/v_{c,o})}; \quad \frac{v_{c,o}}{v_\delta} \left( \frac{v_\delta}{v_1} \right) \frac{\partial\theta_o}{\partial\gamma_o} \frac{\partial(v_1/v_{c,o})}{\partial\gamma_o} (\Delta\gamma_o)^2; \\
 & v_{c,o} \frac{t_\delta}{r_1} \frac{\partial(v_1/v_{c,o})}{\partial\gamma_o} \Delta\gamma_o; \quad \text{and} \quad \left\{ \frac{1}{v_1} \left( \frac{v_1}{v_1} \right)^2 \frac{\partial\theta_o}{\partial\gamma_o} \Delta\gamma_o + \frac{v_e t_\delta}{r_1} \frac{1 - (w_1/w_1) + \ln(w_1/w_1)}{[1 - (w_1/w_1)]^2} \right\} \Delta V_\delta
 \end{aligned}$$

If these terms are neglected equation (B18) becomes

$$\Delta\gamma_1 = \left\{ \frac{T_{c,o}}{V_{c,o}} \frac{1}{1-e} \left[ e - \frac{v_\delta}{v_1} \right] \frac{v_1}{r_1} \frac{\partial(t/T_{c,o})}{\partial(v_o/V_{c,o})} + \frac{1}{V_{c,o}} \frac{v_\delta}{v_1} \frac{\partial\theta_o}{\partial(v_o/V_{c,o})} \right\} \Delta V_o +$$

$$\left\{ T_{c,o} \frac{1}{1-e} \left[ e - \frac{v_\delta}{v_1} \right] \frac{v_1}{r_1} \frac{\partial(t/T_{c,o})}{\partial\gamma_o} + \frac{v_\delta}{v_1} \frac{\partial\theta_o}{\partial\gamma_o} \right\} \Delta\gamma_o + \frac{v_\delta}{v_1} \Delta\varphi +$$

$$\frac{\partial\gamma_\delta}{\partial\omega} \Delta\omega + \frac{\partial\gamma_\delta}{\partial\dot{\gamma}_1} \Delta\dot{\gamma}_1 \tag{B19}$$

The elimination of these terms changes the equation for  $\Delta\gamma_1$  from a nonlinear function of  $\Delta V_o$ ,  $\Delta\gamma_o$ ,  $\Delta V_\delta$ ,  $\Delta\varphi$ ,  $\Delta\omega$ , and  $\Delta\dot{\gamma}_1$  to a linear function of  $\Delta V_o$ ,  $\Delta\gamma_o$ ,  $\Delta\varphi$ ,  $\Delta\omega$ , and  $\Delta\dot{\gamma}_1$ .



APPENDIX C. Evaluation of Partial Derivatives

1. Evaluation of partial derivatives using the ballistic equations

The partial derivatives which will be evaluated using the ballistic

equations are  $\frac{\partial(r_1/r_0)}{\partial(v_0/v_{c,o})}$ ,  $\frac{\partial(r_1/r_0)}{\partial\gamma_0}$ ,  $\frac{\partial(v_1/v_{c,o})}{\partial(v_0/v_{c,o})}$ ,  $\frac{\partial(v_1/v_{c,o})}{\partial\gamma_0}$ ,  $\frac{\partial\theta}{\partial(v_0/v_{c,o})}$ ,  $\frac{\partial\theta}{\partial\gamma_0}$ ,  $\frac{\partial(t/T_{c,o})}{\partial(v_0/v_{c,o})}$ , and  $\frac{\partial(t/T_{c,o})}{\partial\gamma_0}$ .

The forms of the ballistic equations which are of use are listed below.

$$\frac{r_1}{r_0} = \left(\frac{v_0}{v_{c,o}}\right)^2 \cos^2 \gamma_0 \frac{1}{1-e} \quad (A14)$$

$$\frac{v_1}{v_{c,o}} = \frac{1}{\cos \gamma_0} \left(\frac{v_{c,o}}{v_0}\right) (1-e) \quad (A21)$$

$$\theta = \cos^{-1} \frac{1 - (v_0/v_{c,o})^2 \cos^2 \gamma_0}{e} \quad (A23)$$

$$\frac{t}{T_{c,o}} = \frac{1}{2} \left(\frac{v_0}{v_{c,o}}\right)^3 \frac{\cos^3 \gamma_0}{(1-e^2)^{3/2}} \left\{ 1 - \frac{\sqrt{1-e^2}}{\pi} \left[ \frac{2}{\sqrt{1-e^2}} \tan^{-1} \left( \frac{1-e}{1+e} \tan \frac{\pi-\theta}{2} \right) - \frac{e \sin \theta}{1-e \cos \theta} \right] \right\} \quad (A32)$$

$$e = \left\{ 1 + \left(\frac{v_0}{v_{c,o}}\right)^2 \left[ \left(\frac{v_0}{v_{c,o}}\right)^2 - 2 \right] \cos^2 \gamma_0 \right\}^{1/2} \quad (A15)$$

The partial derivatives  $\frac{\partial(r_1/r_0)}{\partial(v_0/v_{c,o})}$ ,  $\frac{\partial(r_1/r_0)}{\partial\gamma_0}$ ,  $\frac{\partial(v_1/v_{c,o})}{\partial(v_0/v_{c,o})}$ ,  $\frac{\partial(v_1/v_{c,o})}{\partial\gamma_0}$ ,  $\frac{\partial\theta}{\partial(v_0/v_{c,o})}$ ,  $\frac{\partial\theta}{\partial\gamma_0}$ ,  $\frac{\partial(t/T_{c,o})}{\partial(v_0/v_{c,o})}$ , and  $\frac{\partial(t/T_{c,o})}{\partial\gamma_0}$  are listed below.

$$\frac{\partial(r_1/r_0)}{\partial(v_0/v_{c,0})} = \frac{2(v_0/v_{c,0})\cos^2 \gamma_0}{(1-e)^2} \left\{ (1-e) + \frac{\cos^2 \gamma_0}{e} \left( \frac{v_0}{v_{c,0}} \right)^2 \left[ \left( \frac{v_0}{v_{c,0}} \right)^2 - 1 \right] \right\} \quad (C1)$$

$$\frac{\partial(r_1/r_0)}{\partial \gamma_0} = - \left( \frac{v_0}{v_{c,0}} \right)^2 \sin 2\gamma_0 \frac{1}{(1-e)^2} \left\{ (1-e) + \frac{\cos^2 \gamma_0}{2e} \left( \frac{v_0}{v_{c,0}} \right)^2 \left[ \left( \frac{v_0}{v_{c,0}} \right)^2 - 2 \right] \right\} \quad (C2)$$

$$\frac{\partial(v_1/v_{c,0})}{\partial(v_0/v_{c,0})} = - \frac{1}{(v_0/v_{c,0})^2 \cos \gamma_0} \left\{ \frac{2 \cos^2 \gamma_0}{e} \left( \frac{v_0}{v_{c,0}} \right)^2 \left[ \left( \frac{v_0}{v_{c,0}} \right)^2 - 1 \right] + (1-e) \right\} \quad (C3)$$

$$\frac{\partial(v_1/v_{c,0})}{\partial \gamma_0} = \frac{(v_0/v_{c,0}) \sin 2\gamma_0}{2e \cos \gamma_0} + \frac{(1-e) \sin \gamma_0}{(v_0/v_{c,0})^2 \cos^2 \gamma_0} \quad (C4)$$

$$\frac{\partial \theta}{\partial \gamma_0} = \frac{(v_0/v_{c,0})^2 \sin 2\gamma_0}{\sqrt{1 - \frac{1}{e^2} \left[ 1 - \left( \frac{v_0}{v_{c,0}} \right)^2 \cos^2 \gamma_0 \right]^2}} \frac{e^2 + \frac{1}{2} \left[ 1 - \left( \frac{v_0}{v_{c,0}} \right)^2 \cos^2 \gamma_0 \right] \left[ \left( \frac{v_0}{v_{c,0}} \right)^2 - 2 \right]}{e^3} \quad (C5)$$

$$\frac{\partial \theta}{\partial(v_0/v_{c,0})} = \frac{2(v_0/v_{c,0}) \cos^2 \gamma_0}{\sqrt{1 - \frac{1}{e^2} \left[ 1 - \left( \frac{v_0}{v_{c,0}} \right)^2 \cos^2 \gamma_0 \right]^2}} \frac{e^2 + \left[ 1 - \left( \frac{v_0}{v_{c,0}} \right)^2 \cos^2 \gamma_0 \right] \left[ \left( \frac{v_0}{v_{c,0}} \right)^2 - 1 \right]}{e^3} \quad (C6)$$

The values of these partial derivatives are presented in figures 2 to 7 as functions of  $(v_0/v_{c,0})$  and  $\gamma_0$ .

The partial derivatives  $\frac{\partial(t/T_{c,o})}{\partial\gamma_o}$  and  $\frac{\partial(t/T_{c,o})}{\partial(V_o/V_{c,o})}$  are developed now. These partial derivatives may be written as

$$\frac{\partial(t/T_{c,o})}{\partial\gamma_o} = \frac{\partial(t/T_{c,o})}{\partial\gamma_o'} + \frac{\partial(t/T_{c,o})}{\partial e} \frac{\partial e}{\partial\gamma_o} + \frac{\partial(t/T_{c,o})}{\partial\theta} \frac{\partial\theta}{\partial\gamma_o} \quad (C7)$$

and

$$\frac{\partial(t/T_{c,o})}{\partial(V_o/V_{c,o})} = \frac{\partial(t/T_{c,o})}{\partial(V_o/V_{c,o})'} + \frac{\partial(t/T_{c,o})}{\partial e} \frac{\partial e}{\partial(V_o/V_{c,o})} + \frac{\partial(t/T_{c,o})}{\partial\theta} \frac{\partial\theta}{\partial(V_o/V_{c,o})} \quad (C8)$$

where  $\gamma_o'$  and  $(V_o/V_{c,o})'$  are dummy variables.

The individual terms of equations (C7) and (C8) are

$$\frac{\partial(t/T_{c,o})}{\partial\gamma_o'} = -3 \tan \gamma_o \left( \frac{t}{T_{c,o}} \right) \quad (C9)$$

$$\frac{\partial(t/T_{c,o})}{\partial(V_o/V_{c,o})'} = 3 \left( \frac{V_{c,o}}{V_o} \right) \left( \frac{t}{T_{c,o}} \right) \quad (C10)$$

$$\frac{\partial(t/T_{c,o})}{\partial e} = \frac{3e}{1-e^2} \left( \frac{t}{T_{c,o}} \right) + \frac{1}{2} \left( \frac{V_o}{V_{c,o}} \right)^3 \frac{\cos^3 \gamma_o}{(1-e^2)^{3/2}} \left[ 1 + \frac{1-e}{1+e} \tan^2 \frac{\pi-\theta}{2} \right]^{-1}.$$

$$\left( \tan \frac{\pi-\theta}{2} \right) \frac{2}{\pi(1+e)^2} \sqrt{\frac{1+e}{1-e}} -$$

$$\frac{(1-e \cos \theta) \left[ (1-e^2)^{1/2} - e(1-e^2)^{-1/2} \right] \sin \theta + (1-e^2)^{1/2} e \sin \theta \cos \theta}{\pi(1-e \cos \theta)^2} \quad (C11)$$

and

$$\frac{\partial(t/T_{c,o})}{\partial\theta} = -\frac{1}{2}\left(\frac{V_o}{V_{c,o}}\right)^3 \frac{\cos^3 \gamma_o}{(1-e^2)^{3/2}} \left\{ \frac{2}{\pi} \left[ 1 + \frac{1-e}{1+e} \tan^2 \frac{\pi-\theta}{2} \right] \sqrt{\frac{1-e}{1+e}} \sec \frac{\pi-\theta}{2} + \frac{(1-e^2)^{1/2} e(\cos \theta - e)}{\pi(1-e \cos \theta)^2} \right\} \quad (C12)$$

Using equation (A15) the terms  $\frac{\partial e}{\partial \gamma_o}$  and  $\frac{\partial e}{\partial (V_o/V_{c,o})}$  are found to be

$$\frac{\partial e}{\partial \gamma_o} = -\frac{1}{2e} \left\{ \sin 2\gamma_o \left(\frac{V_o}{V_{c,o}}\right)^2 \left[ \left(\frac{V_o}{V_{c,o}}\right)^2 - 2 \right] \right\} \quad (C13)$$

and

$$\frac{\partial e}{\partial (V_o/V_{c,o})} = \frac{2 \cos^2 \gamma_o}{e} \left(\frac{V_o}{V_{c,o}}\right) \left[ \left(\frac{V_o}{V_{c,o}}\right)^2 - 1 \right] \quad (C14)$$

The values of  $\frac{\partial(t/T_{c,o})}{\partial \gamma_o}$  and  $\frac{\partial(t/T_{c,o})}{\partial (V_o/V_{c,o})}$  are presented in

figures 8 and 9 as functions of  $\gamma_o$  and  $(V_o/V_{c,o})$ .

2. Evaluation of  $\frac{\partial \gamma_8}{\partial V_8}$ ,  $\frac{\partial \gamma_8}{\partial V_1}$ , and  $\frac{\partial \gamma_8}{\partial \alpha_1}$ .

The change in the flight-path angle during the burning of the last stage ( $\gamma_8$ ) is given by equation (B7) as

$$\gamma = \tan^{-1} \frac{V_8 \sin \alpha_1}{V_1 + V_8 \cos \alpha_1} \quad (B7)$$

This is used to obtain  $\frac{\partial \gamma_\delta}{\partial v_\delta}$ ,  $\frac{\partial \gamma_\delta}{\partial v_1}$ , and  $\frac{\partial \gamma_\delta}{\partial \alpha_1}$ , or

$$\frac{\partial \gamma_\delta}{\partial v} = \frac{v_1 \sin \alpha_1}{v_1^2 + 2v_1 v_\delta \cos \alpha_1 + v_\delta^2} \quad (C15)$$

$$\frac{\partial \gamma_\delta}{\partial v} = - \frac{v_\delta \sin \alpha_1}{v_1^2 + 2v_1 v_\delta \cos \alpha_1 + v_\delta^2} \quad (C16)$$

and

$$\frac{\partial \gamma_\delta}{\partial \alpha} = \frac{v_1 v_\delta \cos \alpha_1 + v_\delta^2}{v_1^2 + 2v_1 v_\delta \cos \alpha_1 + v_\delta^2} \quad (C17)$$

Equations (C15), (C16), and (C17) may be simplified since the angle of attack is sufficiently small so that

$$\begin{aligned} \cos \alpha_1 &\approx 1 \\ &\text{and} \\ \sin \alpha_1 &\approx \alpha_1 \end{aligned}$$

With these approximations the equations become

$$\frac{\partial \gamma_\delta}{\partial v_\delta} = \frac{v_1 \alpha_1}{(v_1 + v_\delta)^2} \quad (C18)$$

$$\frac{\partial \gamma_\delta}{\partial v_1} = - \frac{v_\delta \alpha_1}{(v_1 + v_\delta)^2} \quad (C19)$$

and

$$\frac{\partial \gamma_\delta}{\partial \alpha_1} = \frac{v_\delta}{(v_1 + v_\delta)} \quad (C20)$$

Since  $\alpha_1$  is assumed small, then

$$V_1 + V_8 \approx V_1$$

and,  $\alpha$  may be approximated by

$$\alpha_1 \approx \varphi \approx \frac{\partial \theta}{\partial \gamma_0} \Delta \gamma_0$$

Now equations (18), (C19), and (C20) become

$$\frac{\partial \gamma_8}{\partial V_1} = \frac{1}{V_8} \left( \frac{V_8}{V_1} \right)^2 \frac{\partial \theta}{\partial \gamma_0} \Delta \gamma_0 \quad (C21)$$

$$\frac{\partial \gamma_8}{\partial V_1} = - \frac{1}{V_8} \left( \frac{V_8}{V_1} \right)^2 \frac{\partial \theta}{\partial \gamma_0} \Delta \gamma_0 \quad (C22)$$

and

$$\frac{\partial \gamma_8}{\partial \alpha_1} = \frac{V_8}{V_1} \quad (C23)$$

3. Evaluation of  $\frac{\partial \theta_8}{\partial V_8}$  and  $\frac{\partial \theta_8}{\partial V_1}$ .

The change in central angle ( $\theta_8$ ) during the burning of the last stage may be approximated by assuming that the distance traveled ( $s$ ) is parallel to the local horizontal at the time of the ignition of the last stage. Any change in the altitude during the burning of the last stage will be small compared to the radius and will be neglected. The distance traveled during the burning of the last stage may be found by integration of the classical rocket equation

$$V_i = V_l + V_e \ln \frac{w_l}{w_i} \quad (C24)$$

to yield

$$s = V_l t_\delta + V_e t_\delta \left\{ 1 + \frac{w_l}{w_l - w_i} \ln \frac{w_l}{w_i} \right\} \quad (C25)$$

The angular distance traveled during  $t_\delta$  is

$$\theta_\delta = \tan^{-1} \frac{s}{r_l} \quad (C26)$$

The distance  $s$  is small compared to the radius so that  $\theta_\delta$  may be approximated as

$$\theta_\delta = \frac{s}{r_l} = \frac{V_l t_\delta}{r_l} + \frac{V_e t_\delta}{r_l} \left\{ 1 + \frac{w_l}{w_l - w_i} \ln \frac{w_l}{w_i} \right\} \quad (C27)$$

and thus

$$\frac{\partial \theta_\delta}{\partial V_e} = \frac{V_e t_\delta}{r_l} \frac{1 - (w_l/w_i) + \ln(w_l/w_i)}{[1 - (w_l/w_i)]^2} \quad (C28)$$

and

$$\frac{\partial \theta_\delta}{\partial V_l} = \frac{t_\delta}{r_l} \quad (C29)$$

4. Evaluation of  $\frac{\partial \psi}{\partial t}$  and  $\frac{\partial \theta_{\Delta t}}{\partial t}$ .

In order to evaluate  $\frac{\partial \psi}{\partial t}$  it will be necessary to use the curvature of the ellipse representing the ascent trajectory with no errors and the curvature of the ellipse representing the actual ascent trajectory assuming that near the peak the curvature of these two ellipses are equal.

The equation of an ellipse with the origin at one of the foci is

$$\frac{(x - ae)^2}{a^2} + \frac{y^2}{b^2} = 1 \quad (C30)$$

where  $a$  and  $b$  are the semi-major and semi-minor axes respectively.

This and the other general relations in this section may be found in reference 5. This equation is rewritten in the form

$$y = \frac{b}{a} [a^2 - (x - ae)^2]^{1/2} \quad (C31)$$

The curvature of the ellipse is

$$K = \frac{d^2y}{dx^2} \left\{ 1 + \left( \frac{dy}{dx} \right)^2 \right\}^{-3/2} \quad (C32)$$

When the proper substitutions are made, equation (C32) becomes

$$K = - \frac{(b/a)(x - ae)^2 + (b/a)[a^2 - (x - ae)^2]}{\left\{ [a^2 - (x - ae)^2] + (b/a)^2(x - ae)^2 \right\}^{3/2}} \quad (C33)$$

at the maximum value of  $x(h_A)$

$$x = r_a = a(1 + e)$$

so that the curvature is

$$K = - \frac{a}{b^2} \quad (C34)$$

the relation involving  $a$ ,  $b$ , and  $e$  is

$$b = a(1 - e^2)^{1/2} \quad (C35)$$



so that substitution of (C35) into (C34) yields

$$K = - \frac{1}{a(1 - e^2)} \quad (C36)$$

The injection radius ( $r_1$ ) is

$$r_1 = a(1 + e) \quad (C37)$$

and therefore

$$K = - \frac{1}{r_1(1 - e)} \text{ radians/foot} \quad (C38)$$

When the vehicle is near  $h_A$  the velocity is approximately constant so that

$$\frac{\partial \psi}{\partial t} = v_1 K$$

or

$$\frac{\partial \psi}{\partial t} = - \frac{v_1}{r_1(1 - e)} \text{ radians/sec} \quad (C39)$$

The time rate of change central angle near the peak of the ascent trajectory may be approximated by assuming that the velocity is constant and that the trajectory is a circle of radius  $r_1$ . In this case

$$\frac{\partial \theta_{\Delta t}}{\partial t} = \frac{v_1}{r_1} \quad (C40)$$

#### 5. Evaluation of partial derivatives of apogee and perigee radii.

The equation for the apogee radius is (eq. (A16))

$$\frac{r_a}{r_i} = \frac{(v_i/v_{c,i})^2 \cos^2 \gamma_i}{1 - e} \quad (C41)$$

The injection angle ( $\gamma_1$ ) is almost horizontal ( $\gamma_1 \approx 0$ ) so that  $\cos \gamma_1 \approx 1$  and

$$e \approx \left| \left( \frac{v_1}{v_{c,i}} \right)^2 - 1 \right| \quad (C42)$$

The substitution of equation (C42) into (C41) yields

$$\frac{r_a}{r_1} = \frac{(v_1/v_{c,i})^2}{2 - (v_1/v_{c,i})^2} \quad (C43)$$

and

$$\frac{\partial(r_a/r_1)}{\partial(v_1/v_{c,i})} = \frac{4(v_1/v_{c,i})}{[2 - (v_1/v_{c,i})^2]^2} \quad (C44)$$

An examination of equation (A17) shows that for  $\gamma_1 \approx 0$  the perigee radius is

$$\frac{r_p}{r_1} = \frac{(v_1/v_{c,i})^2}{2 - (v_1/v_{c,i})^2} \quad v_1 \leq v_{c,i} \quad (C45)$$

which is identical to equation (C43). Similarly

$$\frac{\partial(r_p/r_1)}{\partial(v_1/v_{c,i})} = \frac{4(v_1/v_{c,i})}{[2 - (v_1/v_{c,i})^2]^2} \quad v_1 \leq v_{c,i} \quad (C46)$$

If this last equation is evaluated at  $v_1 = v_{c,i}$  it yields

$$\frac{\partial(r_p/r_1)}{\partial(v_1/v_{c,i})} = 4 \quad (C47)$$

The partial derivatives  $\frac{\partial(r_a/r_1)}{\partial\gamma_1}$  and  $\frac{\partial(r_p/r_1)}{\partial\gamma_1}$  must be approximated

since at  $\gamma_1 = 0$  they are both zero. The approximate equations are

$$\frac{\partial(r_a/r_i)}{\partial\gamma_1} \approx \frac{(r_a/r_i)_{\Delta\gamma_1} - (r_a/r_i)_{\gamma_1=0}}{\Delta\gamma_1} \quad (c48)$$

and

$$\frac{\partial(r_p/r_i)}{\partial\gamma_1} \approx \frac{(r_p/r_i)_{\Delta\gamma_1} - (r_p/r_i)_{\gamma_1=0}}{\Delta\gamma_1} \quad (c49)$$

The values of  $\frac{\partial(r_a/r_i)}{\partial(v_i/V_{c,i})}$ ,  $\frac{\partial(r_a/r_i)}{\partial\gamma_1}$ , and  $\frac{\partial(r_p/r_i)}{\partial\gamma_1}$  are presented

in figures 10, 11, and 12. An arbitrary value of  $\Delta\gamma_1 = 2^\circ$  was used

to obtain  $\frac{\partial(r_a/r_i)}{\partial\gamma_1}$  and  $\frac{\partial(r_p/r_i)}{\partial\gamma_1}$ .

#### 6. Evaluation of $\frac{\partial\gamma_8}{\partial\omega}$ and $\frac{\partial\gamma_8}{\partial\dot{\gamma}_1}$ .

These terms involve the changes in the flight-path angle of the spinning last stage during the time it is thrusting and are caused by thrust misalignment and pitching rate at the time of separation of the last stage from the next-to-last stage. The terms are evaluated using information given by the method of Buglia, Young, Timmons, and Brinkworth (ref. 6). These values depend upon the mass and inertia characteristics of the last stage (which are allowed to vary with time), and the spin rate (angular velocity about the axis of symmetry) which is held constant.

A METHOD OF ESTIMATING THE APOGEE AND  
PERIGEE ERROR INCURRED IN ESTABLISHING THE ORBIT  
OF A SPIN-STABILIZED VEHICLE

by

Benjamin J. Garland

ABSTRACT

A necessary part of any study of the performance of a satellite vehicle is an analysis of the effect of errors present during the launching upon the final orbit which is achieved. This information will give the probability of obtaining a specified orbit and will indicate which orbits are practical.

A theory has been developed which predicts the influence of primary errors upon the final orbit of the satellite. The theory was applied to the case of the Scout vehicle for a range of injection altitudes and one payload weight which is representative of the capability of the Scout. It was found that the errors which have the greatest influence on the final orbit of the satellite are the errors in the velocity and flight-path angle at burnout of the last stage, guidance, and thrust misalignment of the last stage.

The results of the study indicate that in the case considered for the Scout the probability of not obtaining an orbit because of errors within the individual tolerances of the system is very small.